

Discovery of CP-690,550: A Potent and Selective Janus Kinase (JAK) Inhibitor for the Treatment of Autoimmune Diseases and Organ Transplant Rejection

Mark E. Flanagan,^{*,†} Todd A. Blumenkopf,[‡] William H. Brissette,[§] Matthew F. Brown,[†] Jeffrey M. Casavant,[†] Chang Shang-Poa,^{||} Jonathan L. Doty,[⊥] Eileen A. Elliott,[†] Michael B. Fisher,[#] Michael Hines,[†] Craig Kent,[†] Elizabeth M. Kudlacz,[‡] Brett M. Lillie,[†] Kelly S. Magnuson,[‡] Sandra P. McCurdy,[†] Michael J. Munchhof,[†] Bret D. Perry,[†] Perry S. Sawyer,[†] Timothy J. Strelevitz,[†] Chakrapani Subramanyam,[†] Jianmin Sun,[†] David A. Whipple,^Δ and Paul S. Changelian[▽]

[†]Groton Laboratories, Pfizer Global Research & Development, Eastern Point Road, Groton, Connecticut 06340, United States,

[‡]Pfizer Global Research & Development, 50 Pequot Avenue, New London, Connecticut 06320, United States, [§]Yale University, New Haven, Connecticut 06520, United States, ^{||}Department of Statistics, University of Connecticut, 215 Glenbrook Road U-4120, Storrs, Connecticut 06269, United States, [⊥]Hill Road, East Lyme, Connecticut 06333, United States, [#]Boehringer Ingelheim Pharmaceuticals, Inc., 900 Ridgebury Road, P.O. Box 368, Ridgefield, Connecticut 06877, United States, ^ΔDel Shankel Structural Biology Center, University of Kansas, 2034 Becker Drive, Lawrence, Kansas 66047, United States, and [▽]Lycera Corporation, 46701 North Commerce Center Drive, Plymouth, Michigan 48170, United States

Received April 7, 2010

There is a critical need for safer and more convenient treatments for organ transplant rejection and autoimmune disorders such as rheumatoid arthritis. Janus tyrosine kinases (JAK1, JAK3) are expressed in lymphoid cells and are involved in the signaling of multiple cytokines important for various T cell functions. Blockade of the JAK1/JAK3-STAT pathway with a small molecule was anticipated to provide therapeutic immunosuppression/immunomodulation. The Pfizer compound library was screened against the catalytic domain of JAK3 resulting in the identification of a pyrrolopyrimidine-based series of inhibitors represented by CP-352,664 (**2a**). Synthetic analogues of **2a** were screened against the JAK enzymes and evaluated in an IL-2 induced T cell blast proliferation assay. Select compounds were evaluated in rodent efficacy models of allograft rejection and destructive inflammatory arthritis. Optimization within this chemical series led to identification of CP-690,550 **1**, a potential first-in-class JAK inhibitor for treatment of autoimmune diseases and organ transplant rejection.

Introduction

Modulation of immune function has been a successful strategy for treating transplant rejection and autoimmune diseases.¹ However, current therapies also possess significant side effects resulting from the ubiquitous expression of their targets of action.² Consequently, researchers continue to search for new biological targets, such as cytokine signaling pathways (one such pathway is shown in Figure 1) that may offer more selective immunosuppressive therapies to treat these conditions.

*To whom correspondence should be addressed. Telephone: 860-441-0205. Fax: 860-715-4693. E-mail: mark.e.flanagan@pfizer.com.

^a Abbreviations: γ_c , γ common chain; ACR, American College of Rheumatology; ADME, absorption, distribution, metabolism, and excretion; 9-BBN, 9-borabicyclo(3.3.1)nonane; BBO, broad band observe; BID, twice daily; CL_R, renal clearance; COSY, correlation spectroscopy; CYP, cytochrome P₄₅₀; DMF, dimethylformamide; DMSO, dimethyl sulfoxide; Fu, fraction unbound; GM-CSF, granulocyte macrophage-colony stimulating factor; GST, glutathione S-transferase; HSA, high-speed analoging; HFF, human foreskin fibroblast; HHT, heterotopic cardiac transplant; HLM, human liver microsome; HMBC, heteronuclear multiple bond coherence; HPLC, high-performance liquid chromatography; HRMS, high-resolution mass spectrometry; HU03, human erythroleukemia cells; iv, intravenous; JAKs, Janus tyrosine kinases; LC/MS/MS, liquid chromatography/tandem mass spectrometry; LRMS, low-resolution mass spectrometry; MMF, mycophenolate mofetil; NADPH, nicotinamide adenine dinucleotide phosphate; NOESY, nuclear Overhauser enhancement spectroscopy; po, orally; RA, rheumatoid arthritis; SAR, structure–activity relationships; SCID, severe combined immunodeficiency; SCX, strong cation exchange; STAT, signal transducers and activators of transcription; THF, tetrahydrofuran; Vd, volume of distribution.

The Janus tyrosine kinases (JAKs)^a have generated great interest in recent years as therapeutic targets due to the unique role that these enzymes play as gatekeepers in the signal transduction process.^{3–5} Named after the Roman god of gates and doors (“Janus”), these four enzymes (JAK1, JAK2, JAK3, and Tyk2) control signaling of numerous cytokines and therefore play a central role in acquired and innate immunity and hematopoiesis.⁶ JAK3 expression is limited to lymphoid cells where it associates with the common γ chain (γ_c) of the IL-2 family of receptors (Figure 1).⁷ JAK1 is broadly expressed, including expression in lymphoid cells as well as the nervous system, where it associates with β -chains of the IL-2 family of receptors, as well as numerous other cytokine receptors. Upon cytokine binding, receptor assembly brings JAK1 and JAK3 in close proximity such that they undergo autophosphorylation and phosphorylation of the β -chain C-terminus. Ultimately, this leads to the activation of signal transducers and activators of transcription (STAT) proteins, a critical step in the relay of messages to the nucleus.⁸ Through this process JAK1 and JAK3 control the signaling pathways of multiple cytokines (IL-2, -4, -7, -9, -15, and -21) important for various T cell functions including development, activation, and homeostasis.⁹ The criticality of these cytokines and the subsequent transduction of their signals for proper T cell function are evident from mutations of JAK3 or γ_c , both of which disrupt cytokine signaling and lead to a virtually identical immunodeficient phenotype [severe combined immunodeficiency

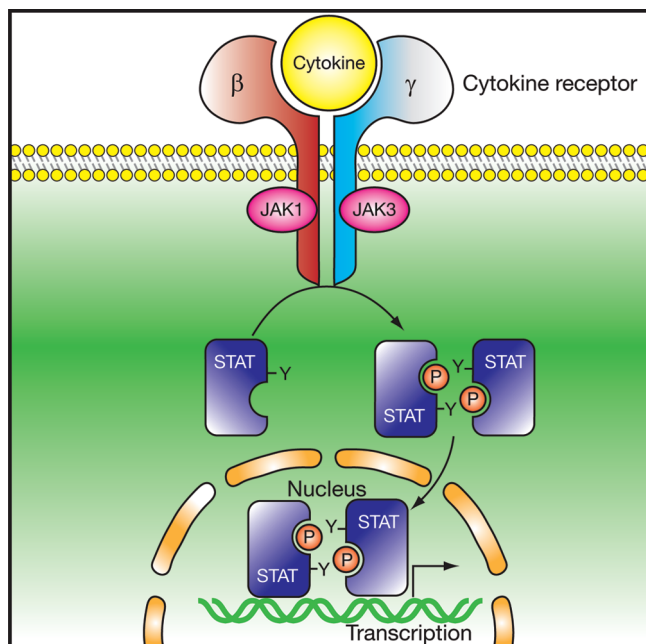


Figure 1. Overview of cytokine signaling through the JAK/STAT pathway. Reprinted by permission from Macmillan Publishers Ltd.: *Nat. Rev. Immunol.* **2003**, 3, 900–911, copyright 2003.

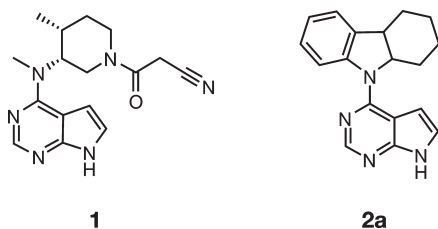


Figure 2. Structure of **1** and HTS lead **2a** (CP-352,664).

(SCID)].^{10–12} Up to two-thirds of all hereditary cases of SCID are believed to occur as a result of mutations in one of these two proteins;¹³ up to 14% of all hereditary cases of SCID are estimated to be due to JAK3 mutations.¹¹

We recognized the potential utility for blockade of this pathway in order to achieve therapeutically desirable immunosuppression/immunomodulation and initiated a program to identify a selective small molecule inhibitor of JAK3. This led to the identification of the development compound CP-690,550 **1** (Figure 2), which has demonstrated efficacy in preclinical and clinical studies of autoimmune diseases, including rheumatoid arthritis (RA) and chronic plaque psoriasis, and renal allograft rejection.^{14–17} We describe herein the medicinal chemistry strategy that led to the discovery of this chemical entity.

Our initial efforts were focused on JAK3 as a target for immunosuppression because its expression is limited to lymphoid cells. To identify lead matter, the Pfizer compound library (~400,000 compounds, ca. 1996) was screened against the JAK3 catalytic domain as a recombinant glutathione *S*-transferase (GST) fusion protein, resulting in the identification of a pyrrolo[2,3-*d*]pyrimidine-containing lead series represented by **2a** (CP-352,664) (210 nM vs JAK3 kinase). Follow-on analogues of **2a** were initially screened against the JAK1, JAK2, and JAK3 enzymes. Inhibition of JAK2 was assessed early in the screening cascade because of its essential role in hematopoiesis, including *epo* receptor signaling and red blood

cell homeostasis,¹² which it was believed could lead to untoward effects such as anemia. Compounds were also evaluated in an IL-2 induced T cell blast proliferation assay, which provides a functional measure of the ability of compounds to inhibit JAK1 and/or JAK3 activities. Additionally, since the lead compound (**2a**) had a short human liver microsome (HLM) half-life (14 min), new analogues were routinely screened for metabolic stability using human liver microsomes for half-life determination.

Cellular specificity assays were also employed for compounds of interest. A human foreskin fibroblast (HFF) assay was used to determine nonspecific inhibition of cellular proliferation outside of the hematopoietic compartment, and a granulocyte macrophage-colony stimulating factor (GM-CSF) induced JAK2 cellular proliferation assay (HU03 cell line) was used to evaluate compounds for JAK2 functional activity. Consequently, a ratio of HU03/IL2-blast activity for a given analogue provided a measure of JAK2 activity relative to JAK1/3. Finally, the most significant *in vivo* hurdle for an experimental immunosuppressive drug was to prolong survival of a transplanted allogeneic organ in a preclinical species. Therefore, select compounds were evaluated in a murine vascularized heterotopic cardiac transplant (HTT) model¹⁴ and a neovascularized transplant model.¹⁸

At the outset of the program the goal was to identify a prototype molecule that had a potency of ≤ 10 nM against the JAK3 kinase and ≤ 100 nM in the IL-2 blast cellular assay, greater than 100-fold selectivity as measured by a comparison of enzyme or cellular data for JAK3 relative to JAK2, HLM half-life nominally of ≥ 60 min, and improved overall physicochemical characteristics relative to **2a**.

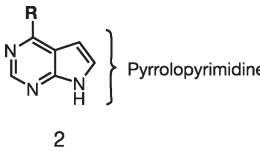
Results

Improved Cellular Potency and the Likely Role of JAK1.

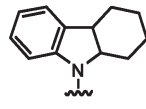
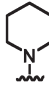
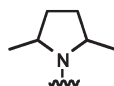
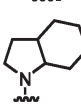
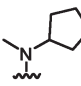
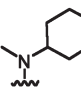
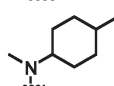
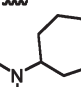
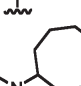
Early structure–activity relationships (SAR) revealed that compounds possessing cyclic, lipophilic, amino headgroups provided the best JAK3 enzyme potency (e.g., **2a–i**, Table 1). Consequently, efforts were focused on optimization of this group from the pyrrolopyrimidine heterocycle in order to achieve the program objectives.

It was anticipated that inhibition of JAK1 could play a role in cellular potency either additively or synergistically with JAK3, due to the manner by which these enzymes operate together at the IL-2 receptor. The first indication of this came from an empirical observation relating amino headgroup structure to IL-2 blast (cell) potency. As illustrated in Table 1, it was observed that compounds possessing an *N*-methyl-cycloalkyl headgroup motif exhibited an improvement in cell potency. This was unexpected based solely on consideration of JAK3 potency, which remained approximately the same as compared with earlier compounds (e.g., **2a–c**). However, the *N*-methyl-cycloalkyl analogues demonstrated greater potency against JAK1 (e.g., **2e–i**), suggesting that the combination of JAK1 and JAK3 (or JAK1 alone) may be key to realizing the improved cellular potencies observed. The physical property (clogP) distribution across these compounds (**2**) and the fact that none were crystalline when initially tested make other explanations for these cellular potency differences, such as solubility or plasma protein binding, less likely. The role of JAK1 is further supported by the fact that **1** in a solution phase kinase assay was more potent against JAK1 than measured in the ELISA assay (IC_{50} = 3.2, 4.1, and 1.6 for JAK1, JAK2, and JAK3, respectively).¹⁹ This latter

Table 1. Headgroup Structure and JAK Enzyme Potencies of Compounds **2a–2i**^a



2

Compound	Headgroup (R)	JAK3 IC ₅₀ (nM)	JAK2/ JAK3	JAK1 IC ₅₀ (nM)	Cell IC ₅₀ (nM)	clogP	HLM t _{1/2} (min)
2a		210	45	> 10000	3200	4.77	15
2b		210	6	> 10000	3900	1.99	16
2c		270	1.4	>10000	4250	2.47	ND
2d		350	7.8	1760	330	2.86	8
2e		390	4	670	280	2.79	20
2f		160	9	1700	390	3.34	12
2g		370	3	720	330	3.86	27
2h		110	0.3	1200	310	3.90	14
2i		58	3	2240	650	4.46	7

^a Cell potencies were determined using an IL-2 induced T cell blast proliferation assay. Metabolic stabilities of **2a–2i** were determined by incubations with human liver microsomes (HLMs) and reported by half-life.

point will be explored in more detail in the Discussion and Conclusions.

While the *N*-methyl-cycloalkyl analogues (**2e–i**) demonstrated improved whole-cell activity compared with the lead (**2a**), the JAK2/JAK3 selectivity did not improve. Furthermore, these analogues showed no improvement in metabolic stability as indicated by their HLM half-lives. Therefore, many issues remained, but further investigation was warranted based on the association of this SAR with improved cellular potency. We expanded on this SAR through the use of high-speed analoging (HSA) as illustrated in Figure 3.

Reductive aminations with methylamine were conducted with cyclic ketones containing various functionalities. The resulting cyclic amines (**4**) were then coupled to the 4-chloropyrrolopyrimidine (**5**), purified, and tested. In all, approximately 100 compounds (**6**) were targeted in this manner. Polar features were included in this array in an effort to improve metabolic stability and physical properties. Unfortunately, the randomized placement of these polar groups in this experiment resulted only in compounds exhibiting reduced

kinase activity (see also Supporting Information Table 1). Although a breakthrough in combining metabolic stability with improved cellular potency was not realized, other important SAR features were revealed from this HSA study. Compounds **6a–c** indicated a potency advantage for methyl substitutions at the C2' and/or C5' positions of a cyclohexane ring; the most potent compound identified was **6c**, which exhibited a 2',5'-dimethyl substitution pattern on the cyclohexyl ring. At 20 nM potency against JAK3, even as a mixture of at least three isomers (prepared from the racemic ketone), this material represented an 8-fold improvement in JAK3 inhibition compared with **2f** (unsubstituted cyclohexyl). Although the cellular potency for these did not reflect this 8-fold difference, JAK1 enzyme data were not determined for these HSA compounds, which may have helped to explain this discrepancy. As shown for the other compounds in Figure 3, a small substituent at C2' (methyl or ethyl) provided the most significant potency boost. Although a small substituent at this position was clearly advantageous, larger groups were not well tolerated (e.g., **6e–h**). While

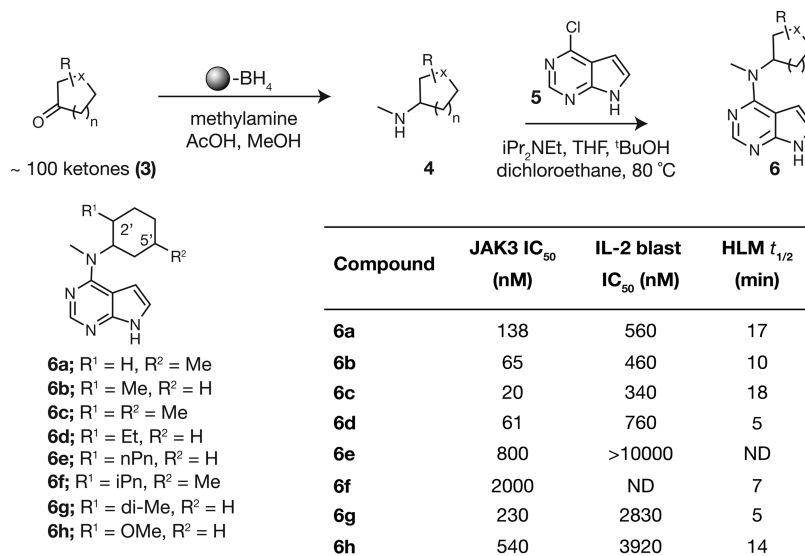
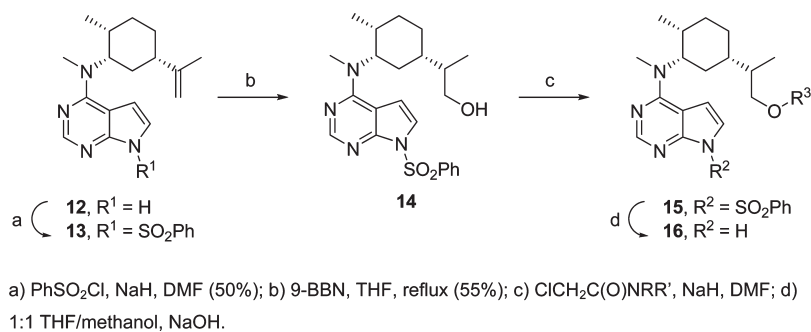


Figure 3. Expansion of structure–activity relationships using high-speed analoging around the *N*-methyl-cycloalkyl headgroup motif leading to compounds **6a–h**.

Table 2. HSA Follow-Up Compounds Derived from Carvone Analogue **12**



Compound	R ³	JAK3 IC ₅₀ (nM)	JAK2/JAK 3	IL-2 blast IC ₅₀ (nM)	clogP	HLM t _{1/2} (min)
16a	-H	20	0.75	225	3.32	13
16b		32	15	630	4.51	5
16c		38	8	420	3.02	29
16d		13	15	190	4.73	3
16e		150	13	150	5.56	5

SAR at the C2' position appeared to be restricted to smaller groups, HSA follow-up compounds derived from the natural product carvone (described in the next section) indicated that the C5' position would accommodate larger groups (Table 2).

Optimizing Interactions through the Use of Natural Products. One follow-up strategy employed to capitalize on learnings from the HSA work and potentially to simplify the stereochemical issues associated with the **6c** mixture was to take advantage of natural products that offered access to similarly substituted ring systems as exhibited by **6c**. One such natural product was carvone (**7**, Figure 4). Carvone is a member of the terpenoid family, and in addition to possessing

the desired substitution around the cyclohexane ring, it also offered the advantage of being commercially available in both the *R*-(−) and *S*-(+) stereochemical configurations.²⁰ Therefore, as illustrated in Figure 4, reduction of the carvone double bond with L-selectride, followed by reductive amination with methylamine, generated a mixture of the amine isomers **9**. Reacting mixture **9** with **5** resulted in new mixtures that were approximately 1:1 consisting of the all-*cis* and all-equatorial products. Remarkably, the mixture derived from *S*-(+)-carvone (**11**) was approximately 300 times more potent against JAK3 kinase than the corresponding mixture derived from *R*-(−)-carvone (**10**). Separation and analysis of

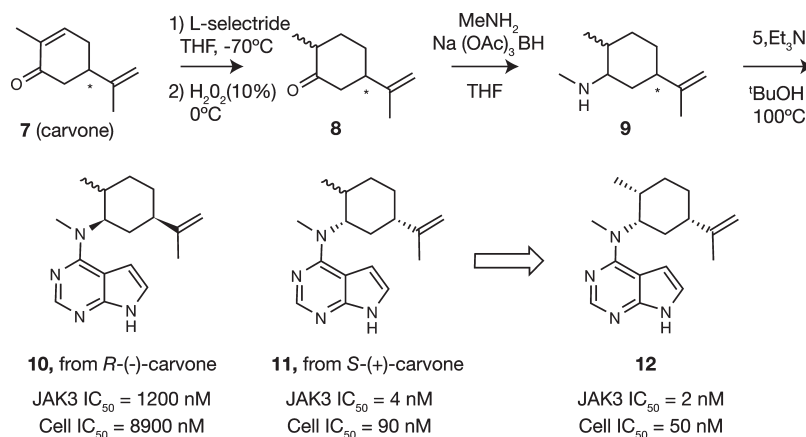


Figure 4. Generation of carvone-derived analogues resulting in the identification of milestone compound **12**.

Table 3. Moving from the Carvone Analogues to a Piperidine-Containing Headgroup Scaffold^a

Compound	R ²	JAK1 IC ₅₀ (nM)	JAK2 IC ₅₀ (nM)	JAK3 IC ₅₀ (nM)	JAK2/ JAK 3	Cell IC ₅₀ (nM)	HLM <i>t</i> _{1/2} (min)
17a sulfonamide		2780	790	14	56	1260	29
17b urea		1120	510	26	20	180	43
17c amine		> 10000	1,440	42	34	1270	19
17d amide		840	480	32	15	450	> 120

^aThe main subseries investigated were sulfonamides, ureas, amines, and amides (representative examples).

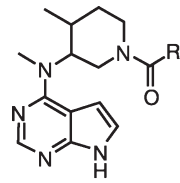
the components of **11** revealed that the all-*cis* compound **12** was the most potent isomer (JAK3 IC_{50} = 2 nM; IL-2 blast IC_{50} = 50 nM), therefore establishing the optimal relative and absolute stereochemistry around the cyclohexane ring to be the all-*cis* configuration derived from *S*-(+)-carvone. Importantly, **12** represented a milestone for the program, as it was the first analogue tested that possessed both JAK3 kinase and cellular potencies consistent with program objectives. With greater hydrophobicity (a higher clogP) than **6c**, it was not surprising that microsomal stability for **12** was poor (HLM $t_{1/2}$ = 14 min). Furthermore, aqueous solubility (1.3 $\mu\text{g/mL}$) and rat bioavailability (% F ~ 7) were less than desirable.

Attempts to address these issues from this carvone scaffold resulted in some potent analogues (e.g., Table 2); however, it was ultimately determined that the lipophilicity of the core cyclohexane ring of this series made it difficult to address pharmacokinetic issues while maintaining other desirable attributes. Furthermore, many of the synthetic manipulations from the isopropenyl group of **12** resulted in a new stereocenter, which complicated analogue generation and scale-up.

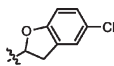
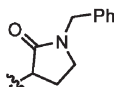
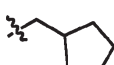
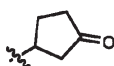

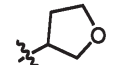
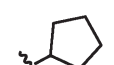
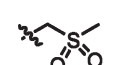
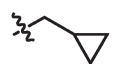
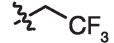

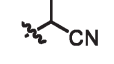

Consequently, our strategy shifted toward identifying more polar headgroups capable of providing analogues in more drug-like space ($\text{clogP} \leq 3$).

Improved Properties: The “Piperidine Series” and 1. To address issues with the carvone analogues, we moved to a piperidine headgroup scaffold as illustrated in Table 3. The advantages of adding a heteroatom into the cyclohexane ring were several. First, this change lowered the clogP of the target compounds compared with similar carvone-derived analogues (generally greater than one logP unit). Second, incorporating a nucleophilic nitrogen at this position in the ring (at what would be the C5' position of a cyclohexyl) greatly facilitated analogue generation by allowing attachment of groups through a variety of linkages. Finally, by preparing compounds in this manner, it was possible to avoid the introduction of the additional stereocenters generated through modification of the carvone isopropenyl group. Although the piperidine had two stereocenters that required being appropriately defined and set, this was eventually accomplished very efficiently by classical resolution (patent WO 096909, 2002).²¹

Table 4. Structure–Activity Relationships for the Amide Subseries of Piperidine-Containing Compounds



18

Compound	Structure R	JAK3 IC ₅₀ (nM)	JAK2/ JAK 3	JAK1 IC ₅₀ (nM)	Cell IC ₅₀ (nM)	clogP	HLM t _{1/2} (min)
18a		480	> 20	ND	3300	4.50	4
18b		117	26	>7140	1400	3.40	ND
18c		230	> 25	ND	2500	3.67	ND
18d		29	28	1550	335	1.81	30
18e		143	20	>10000	2510	2.99	21
18f		40	26	>10000	2500	2.01	91
18g		39	25	ND	320	3.05	ND
18h		147	8.3	>10000	2410	1.01	>120
18i		20	23	1910	230	2.55	14
18j		19	23	1480	210	2.37	60
18k		113	23	>7500	1400	2.14	30
18l		13	21	490	140	1.83	83
18m		3.3	20	110	40	1.52	> 100

Given the tight SAR observed for the carvone-derived analogues, the fundamental question at the outset of the piperidine approach was whether it would be possible to introduce a heteroatom into this ring and still maintain desirable enzyme and cellular potency. To address this question, a variety of groups were appended to the piperidine. The main subseries investigated were sulfonamides, ureas, amines (reductive amination products), and amides (Table 3). Although the SAR varied across these subseries, the important general finding was that good JAK3 enzyme potency was achievable from this scaffold. Sulfonamides provided good JAK3 inhibition and encouraging selectivity relative to JAK2, but cell potency was found to be very difficult to achieve. Several urea analogues exhibited very good potency (both enzyme and cell); however, finding the right balance of other properties

proved difficult. Several analogues with alkyl group substitutions on the piperidine nitrogen provided excellent enzyme potency but required electron-withdrawing groups (benzylic) in order to reduce the pK_a of the piperidine nitrogen (ionization in the headgroup typically resulted in significant loss of activity). These lipophilic amines generally exhibited high plasma protein binding and significant HLM metabolism.

The amide subseries was ultimately successful (Table 4). One early trend observed with these amide-containing compounds was that smaller substituents generally conferred better enzyme potency; furthermore, the cell potency tracked with an amalgamation of JAK3 and JAK1 enzymatic inhibitions. Importantly, these compounds also followed a trend for lower clogPs (≤ 2) translating to improved metabolic stability. As a consequence, the cyanoacetamide compound

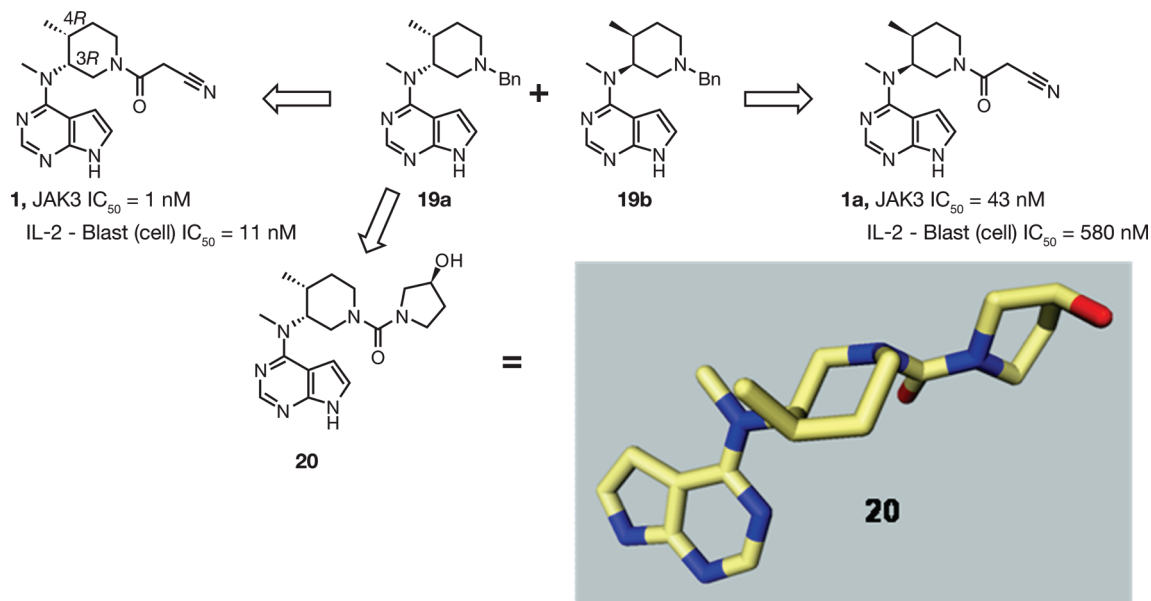


Figure 5. Preparation of both enantiomers of **1** from intermediates **19a** and **19b**, separated by chiral HPLC. Single crystal X-ray structure of urea analogue **20**, prepared from **19a**, provided unambiguous confirmation of the 3*R*,4*R* stereochemical configuration for **1**.

18m was prepared, as it was anticipated that the small, polar nature of this side chain would intersect both of these SAR patterns and impart improved potency and metabolic stability. This is precisely what was observed, and with **18m**, for the first time, all *in vitro* program objectives had been met, with the exception of selectivity for JAK3 over JAK2, which was still measured to be only 20-fold.

Separation of the enantiomers of **18m** was not successful by chiral high-performance liquid chromatography (HPLC); however, the benzyl-protected precursor of this material (**19**) was separable by this method (Figure 5). The two purified components **19a** and **19b** were therefore carried forward separately producing **1** and its enantiomer **1a**. Evaluation of these two compounds revealed that **1** had an IC_{50} of 1 nM against JAK3, which was approximately 40 times more potent than **1a**. Eventually all four stereoisomers of **18m** were prepared and studied in our laboratories and other laboratories.²² With compound **1** being the most potent isomer it was anticipated that its absolute stereochemical configuration would reflect that of the most potent carvone-derived analogue **12**. Final stereochemical confirmation for **1** came from the evaluation of a related urea analogue **20** (Figure 5). Compound **20** was crystalline as the free base, and since the stereochemical configuration of the pyrrolidinol moiety was known (derived from (*S*)-3-hydroxypyrrolidine), the corresponding single crystal X-ray structure of **20** provided unambiguous assignment of the 3*R*,4*R* stereochemical configuration for **1**. Corroboration of this stereochemical assignment has come from published cocrystal structures of **1** with JAK family members.^{23,24}

In order to proceed to development studies, a suitable solid form of **1** needed to be identified. To do this, the free base of **1** was screened against a panel of acids, resulting in the identification of the crystalline citrate salt. This material (citrate salt) was ultimately selected for development based on its desirable characteristics of good solubility (>4 mg/mL in water), high melting point onset (>200 °C), lack of hygroscopicity, and high degree of crystallinity (patent WO 048162, 2003).²⁵

Preclinical Pharmacokinetics. **1** is being developed as the crystalline citrate salt. In rats and dogs, intravenous (iv)

dosing of **1** resulted in moderate to high plasma clearances, which were predicted from microsome incubations ($t_{1/2}$ = 68 and 30, respectively). In monkeys, plasma clearances were low to moderate, consistent with the half-life observed in monkey liver microsomal incubations (>100 min). Low to moderate volumes of distribution were also observed, resulting in half-lives of 0.6–2.1 h (Table 5). Oral dosing of the crystalline citrate salt resulted in oral bioavailabilities that were consistent with the expected magnitude in first-pass hepatic metabolism, estimated from the iv clearances. Plasma protein binding for **1** was very similar in rats, dogs, monkeys, and humans [human fraction unbound (Fu) = 24%]. Preliminary *in vitro* studies predicted minimal risk with respect to unwanted drug–drug interactions for multiple cytochrome P₄₅₀ (CYP) isoforms (IC_{50} s > 52 μ M for CYPs 1A2, 2C19, 2D6, and 3A4). Studies performed in Caco-2 cell monolayers predicted that **1** (at 10 μ M) should not be a substrate for efflux transporters and should be absorbed transcellularly by passive diffusion with a predicted human absorption of >70%.

In contrast to the moderate to high clearances observed in preclinical species, human hepatic metabolism of **1** was predicted to be low based on studies conducted in human liver microsomes and hepatocytes ($t_{1/2}$ > 120 min). Consequently, the low clearance of the citrate salt in humans was predicted to occur via a combination of renal excretion of unchanged drug and low hepatic metabolic clearance. Allometric scaling of the renal clearance (CL_R) in animals (Table 5) yielded a predicted human CL_R of 1.2 mL min^{−1} kg^{−1}, which was then incorporated with an estimate of low metabolic clearance (≤ 2.5 mL min^{−1} kg^{−1}). Volume of distribution predictions yielded an average V_{dss} in human of 1.9 L/kg. Based on the V_{dss} and CL predictions, the predicted terminal elimination half-life in human was ~7 h. Therefore, although **1** was metabolized in preclinical species, the low metabolic turnover observed with human liver microsomes and hepatocytes provided confidence that clearance would occur predominantly via a combination of renal excretion of unchanged drug and low hepatic metabolic clearance, and pharmacokinetics sufficient to support qd or bid dosing of **1** would be observed in humans. This prediction has largely held true in the clinic

Table 5. Preclinical Pharmacokinetic (PK) Summary for **1**

species	iv PK summary					po PK summary		
	CL (mL min ⁻¹ kg ⁻¹)	CL _R (mL min ⁻¹ kg ⁻¹)	Vdss (L/kg)	t _{1/2} (h)	Fu (%)	dose (mg/kg)	C _{max} (ng/mL)	F (%)
rat	62	6.2	2.6	0.6	23	10	442	27
dog	19	1.9	1.8	1.2	19	5	1020	78
monkey	18	2.3	1.7	2.1	26	5	790	48

(oral $t_{1/2}$ = 2–5 h) with the exception that some hepatic metabolism of **1** was in fact observed via CYPs 3A4/5 and 2C19.^{26–28}

Discussion and Conclusions

Following its identification as a lead molecule, the *in vitro* pharmacology of **1** has been studied extensively. The results of these studies show **1** to be a potent inhibitor of the JAK kinase family, with a high degree of selectivity within the human kinome.²⁹ Structural and thermodynamic characterization of **1** complexed with JAK family members provides insights into this high degree of kinome selectivity.²⁴

Previous reports of kinase activity describe **1** as being 20-fold selective relative to JAK2 and 112-fold selective relative to JAK1.¹⁴ More recently, in solution-phase caliper assays **1** exhibited low nanomolar “PAN” inhibitory potency against JAK1, JAK2, and JAK3 and to a lesser extent Tyk2 (IC₅₀ = 3.2, 4.1, 1.6, and 34.0 for JAK1, JAK2, JAK3, and Tyk2, respectively).¹⁹

In cellular assays **1** exhibited 11 nM potency in the IL-2 blast proliferation assay (JAK1 and JAK3), 324 nM potency in the HU03 cellular specificity assay (JAK2), and >10000 nM activity in the HFF assay (nonspecific effects on cellular proliferation).¹⁴ While the JAK kinase activities for **1** changed with assay conditions, the cellular potencies measured are consistent with recent results of a human whole blood assay indicating that γ_c cytokine-dependent activation (driven by JAK1 and JAK3) was potentially inhibited by **1**, exhibiting functional selectivity over GM-CSF-dependent (JAK2-driven) activation of the pathway.^{19,30}

These data confirm that the desired 100-fold selectivity for JAK3 relative to the other JAKs was ultimately not accomplished with **1**; however, inhibition of JAK1 and JAK2 may actually enhance the efficacy of **1** for certain indications, such as RA, by impeding the signaling of proinflammatory cytokines, such as IL-6 (IL-6 signals through JAK1/JAK2). It is therefore possible that a near-optimal balance of JAK kinase inhibitions may have fortuitously been achieved with **1**, benefiting efficacy across multiple therapeutic indications while maintaining clinically manageable functional selectivity for JAK2.

Clinical Development. **1** is currently in clinical development for RA (phase III), prevention of acute (renal) allograft rejection (phase II), psoriasis (oral and topical; phase II), Crohn’s disease (phase II), ulcerative colitis (phase II), and dry eye disease (topical; phase I/II).

In preclinical studies of inhibition of allograft rejection **1**, dosed as monotherapy or in combination with mycophenolate mofetil (MMF), demonstrated efficacy in rodents and in nonhuman primates; prolonged survival was observed in a dose-responsive fashion.^{14,31} Prevention of allograft rejection has also been demonstrated in a rat model of aorta transplantation³² and in various other murine models.¹⁸

Following the encouraging findings in preclinical transplant models, **1** was evaluated in renal allograft recipients. The tolerability profile of **1** coadministered with MMF was evaluated in a phase I dose-escalation study.²⁶ In a pilot, phase IIa multi-

center study, **1** dosed at 15 and 30 mg bid was compared with tacrolimus in 61 patients receiving *de novo* kidney transplants.³³

In the latter study, immune suppression in the **1** treatment groups was supported by prevention of rejection and by evidence of infection. The effects of JAK2 may have manifested in the **1** groups as a trend toward more frequent anemia and neutropenia. This study suggests that relatively low rates of acute rejection are achievable with **1**-based regimens and that JAK inhibition provides a novel, potentially viable means to prevent allogeneic response in allograft recipients.

1 has also demonstrated efficacy in therapeutic models of destructive, inflammatory arthritis in rodents.³⁴ Encouraged by these data, **1** entered development as a disease-modifying antirheumatic drug (DMARD) for the treatment of RA. A 6-week proof-of-concept study in 264 adult patients with active RA, who had an inadequate response to methotrexate, etanercept, infliximab, or adalimumab, compared **1** (5, 15, and 30 mg bid) with placebo. All three doses resulted in significant improvement versus placebo ($p < 0.0001$) in the primary end point, American College of Rheumatology (ACR)20.³⁵ In this study, the most common adverse events reported were headache and nausea. The risk of infection over 6 weeks appeared to be slightly higher for **1** 15 and 30 mg bid than placebo or **1** 5 mg bid. Dose-dependent decreases in absolute neutrophil count and a dose response in mean change (decrease) from baseline in hemoglobin were observed. Small increases (0.004–0.06 mg/dL mean) in mean serum creatinine compared with baseline and with placebo and dose-dependent increases in total, high-density lipoprotein—and low-density lipoprotein—cholesterol were observed in all **1** dose groups.³⁵

This study was followed by two large phase IIb placebo-controlled, dose-ranging studies, one in 509 RA patients with an inadequate response to stable background methotrexate (study A3921025; NCT00413660^{36,37}) and one in 384 patients with an inadequate response to prior DMARDs, who had discontinued all traditional and biologic DMARDs other than antimalarials (study A3921035; NCT00550446^{38,39}). Study A3921035 also included adalimumab dosed 40 mg subcutaneously every other week for six injections, followed by **1** 5 mg bid for another 12 weeks.

In the analysis of the primary end points in studies A3921025 and A3921035, **1** [3–15 mg bid; 20 mg qd (A3921025 only)] was significantly effective for the primary end point, ACR20 response at 12 weeks compared with placebo. Adverse events in both studies were similar to those observed in other phase II studies; in addition, a slight increase in the rate of alanine aminotransferase increases >3 times the upper limit of normal was observed in patients dosed with **1** 15 mg bid in study A3921025.³⁶

Phase III studies of **1** (5 and 10 mg bid) for the treatment of RA, a phase II study (2, 5, and 15 mg bid) for psoriasis, and a phase I/II study (topical solution) are currently ongoing.

In conclusion, the JAK1/3-STAT signaling pathway has proven to be a highly potent and productive target for selective immunosuppression/immunomodulation. The utility of exploiting this mechanism is evident from the preclinical and

clinical efficacy observed with **1**. JAK3 was the original target due to its expression being limited to lymphoid cells and the immunosuppressed phenotype of patients possessing mutations in this protein. While the targeted 100-fold selectivity for JAK3 relative to JAK2 was ultimately not achieved, **1** is highly selective for the JAK family of kinases. Furthermore, in cellular assays, **1** has demonstrated functional selectivity for JAK1/3 versus JAK2, which importantly has proven to be manageable clinically in terms of unwanted JAK2 effects, such as anemia, aided by the favorable pharmacokinetics of this compound.

To find this chemical entity, a standard high-throughput screening protocol was initiated, which resulted in the identification of **2a**. With this lead, a strategy was pursued in which the basic medicinal chemistry principles of low molecular weight and logP were observed, eventually leading to a highly soluble, highly ligand and lipid efficient inhibitor in **1**. From the outset of the program the issues of potency (both enzyme and cell), metabolic stability, and selectivity were engaged simultaneously. High-speed analoging was performed to screen chemical space quickly, resulting in new substitution patterns associated with potency improvements. Natural products were also used as chemical building blocks to understand target binding better and to optimize interactions. Finally, a scaffold shift to a piperidine-containing headgroup resulted in an improvement in drug-like properties. Ultimately, however, it was the introduction of the cyanoacetamide side chain that brought the optimal balance of potency, chemical properties, and pharmacokinetic attributes that has positioned **1** to become a novel, first-in-chemotype, and potential first-in-class JAK inhibitor for the treatment of autoimmune diseases and organ transplant rejection.

Experimental Section

Enzyme Assays. The JAK1, JAK2, and JAK3 kinase assays utilize a protein expressed in baculovirus-infected SF9 cells (a fusion protein of GST and the catalytic domain of human JAK enzyme) purified by affinity chromatography on glutathione-Sepharose. The substrate for the reaction was polyglutamic acid-tyrosine [PGT (4:1), Sigma catalog no. P0275], coated onto Nunc Maxi Sorp plates at 100 μ g/mL overnight at 37 °C. The plates were washed three times, and JAK enzyme was added to the wells, which contained 100 μ L of kinase buffer (50 mM HEPES, pH 7.3, 125 mM NaCl, 24 mM MgCl₂) + ATP + 1 mM sodium orthovanadate. After incubation at room temperature for 30 min, the plates were washed three times. The level of phosphorylated tyrosine in a given well was determined by standard ELISA assay utilizing an anti-phosphotyrosine antibody.

Cell Assays. Inhibition of Human IL-2 Dependent T Cell Blast Proliferation (IL-2 Blast Assay). This screen measures the inhibitory effect of compounds on IL-2 dependent T cell blast proliferation *in vitro*. Since signaling through the IL-2 receptor requires JAK3, cell active inhibitors of JAK3 should inhibit IL-2 dependent T cell blast proliferation. The cells for this assay are isolated from fresh human blood. After separation of the mononuclear cells using Accuspin System-Histopaque-1077 (Sigma catalog no. A7054), primary human T cells are isolated by negative selection using Lympho-Kwik T (One Lambda, Inc., catalog no. LK-50T). T cells are cultured at $(1-2) \times 10^6$ /mL in media [RPMI + 10% heat-inactivated fetal calf serum (Hyclone catalog no. A-1111-L) + 1% penicillin/streptomycin (P/S; Gibco)] and induced to proliferate by the addition of 10 μ g/mL PHA (Murex Diagnostics, catalog no. HA 16). After 3 days at 37 °C in 5% CO₂, cells are washed three times in media and resuspended to a density of $(1-2) \times 10^6$ cells/mL in media plus 100 units/mL

human recombinant IL-2 (R&D Systems, catalog no. 202-IL). After 1 week the cells are IL-2 dependent and can be maintained for up to 3 weeks by feeding twice weekly with equal volumes of media plus 100 units/mL IL-2.

To assay for a test compound's ability to inhibit IL-2 dependent T cell proliferation, IL-2 dependent cells are washed three times, resuspended in media, and then plated (50000 cells per well/0.1 mL) in a flat-bottom 96-well microtiter plate (Falcon catalog no. 353075). From a 10 mM stock of test compound in dimethyl sulfoxide (DMSO), serial 2-fold dilutions of compound are added in triplicate wells starting at 10 μ M. One row serves as 100% proliferation control and is incubated with DMSO alone. After 1 h, 10 units/mL IL-2 is added to each test well, and plates are then incubated at 37 °C and 5% CO₂ for 72 h. Plates are then pulsed with [³H]thymidine (0.5 μ Ci/well; NEN catalog no. NET-027A) and incubated for an additional 18 h. Culture plates are harvested with a 96-well plate harvester, and the amount of [³H]thymidine incorporated into proliferating cells is determined by counting on a Packard Top Count scintillation counter. Data are analyzed by plotting the percent inhibition of proliferation versus the concentration of test compound. An IC₅₀ value (micromolar) is determined from this plot.

Inhibition of Human Erythroleukemia Cells (HU03 Assay).

This screen is designed to assess the ability of compounds to inhibit GM-CSF-driven proliferation of the human erythroleukemia cell line HU03. GM-CSF receptor is dependent upon the protein tyrosine kinase JAK2 for signaling. This screen assesses the cellular activity of compounds that inhibit this kinase. HU03 are maintained [RPMI + 10% FCS + P/S + 25 ng/mL GM-CSF (Sargramostim Leukine, 250 μ g; Immunex Corp.)] at $3.5 \times 10^5 - 1.0 \times 10^6$ cells/mL. The cells are fed three times per week depending upon the cell count. To assay for a test compound's ability to inhibit GM-CSF-dependent HU03 cell proliferation, cells are washed three times, resuspended in media, and then plated (2500 cells per well/0.1 mL) in a flat-bottom 96-well microtiter plate (Falcon catalog no. 353075). From a 10 mM stock of test compound in DMSO, serial 2-fold dilutions of compound are added in triplicate wells starting at 10 μ M. One row serves as 100% proliferation control and is incubated with DMSO alone. After 1 h, 50 μ L of 10 units/mL GM-CSF (final) in media is added to all wells. Plates are then incubated at 37 °C and 5% CO₂ for 72 h. Cells are pulsed with [³H]thymidine and harvested, and percent inhibition is determined in the same fashion as the IL-2 dependent T cell proliferation assay.

Inhibition of Human Foreskin Fibroblast Proliferation (HFF Assay).

This screen measures nonspecific inhibition of cellular proliferation. HFFs are obtained from explants of neonatal human foreskin tissue and cultured in media (DMEM with 10% heat-inactivated fetal bovine serum and 1% P/S). Primary cultures are grown in media in tissue culture flasks and split prior to confluency using trypsin-EDTA (Gibco). Fibroblasts are grown in T-175 tissue culture flasks and split 1:5 every 3-4 days. HFFs are used in this assay from passage 5 to 16. To assay for a test compound's ability to inhibit HFF proliferation, cells are trypsinized and washed three times, resuspended in media, and then plated (2500 cells per well/0.15 mL) in a flat-bottom 96-well tissue culture plate (Falcon catalog no. 353075). From a 10 mM stock of test compound in DMSO, serial 2-fold dilutions of compound are added in triplicate wells starting at 10 μ M. One row is plated with DMSO only and serves as the 100% proliferation control. Cells are pulsed with [³H]thymidine and harvested, and percent inhibition is determined in the same fashion as the IL-2 dependent T cell proliferation assay.

In Vitro Pharmacokinetic Assays. *In vitro* absorption, distribution, metabolism, and excretion (ADME) and *in vivo* studies were carried out in accordance with previously published methods.⁴⁰

Microsome Incubations. Incubations of **1** (1 μ M) were carried out in replicate with microsomes (CYP concentration = 0.25 μ M) in 0.1 M potassium phosphate buffer (pH = 7.4) at 37 °C. The reaction mixture was prewarmed at 37 °C for 2 min

before adding nicotinamide adenine dinucleotide phosphate (NADPH) (1.2 mM). The final incubation volume was 600 mL. Aliquots (75 mL) of the reaction mixture at $t = 0, 2, 5, 15$, and 30 min were added to acetonitrile (200 mL) containing indomethacin as internal standard (50 ng/mL), and the samples were centrifuged at 2500g for 5 min before liquid chromatography/tandem mass spectrometry (LC/MS/MS) analysis. For control experiments, NADPH was omitted from these incubations.

Hepatocyte Incubations. Stability of **1** in hepatocytes was examined as follows. Cryopreserved hepatocytes from preclinical species and human were thawed and suspended in Williams' E media supplemented with 24 mM sodium bicarbonate and 10% fetal bovine serum at 0.5×10^6 viable cells/mL for clearance prediction. **1** (1 μ M) for clearance predictions was incubated with hepatocytes at 37 °C for 4 h with gentle agitation. A gas mixture of oxygen/carbon dioxide (95:5) maintained at about 2.5 kPa for about 5 s was passed through this mixture at every 1 h of incubation. Flasks were corked immediately after gassing. Freezing the incubation aliquots in liquid nitrogen terminated the reactions. Following extraction, the samples were then analyzed by LC/MS/MS.

Plasma Protein Binding. The binding of **1** to rat, dog, monkey, and human plasma proteins was determined using the equilibrium dialysis method. **1** was added to fresh plasma from animals or human. **1** concentrations examined are pharmacologically relevant based on *in vivo* efficacy studies in animals. The plasma samples (1 mL) were subjected to equilibrium dialysis ($n = 6$ or 8) using Spectra Por dialysis membranes (VWR, West Chester, PA, USA) with a molecular mass cutoff of 12.4 kDa. The resulting plasma samples were subjected to dialysis against isotonic phosphate buffer (pH 7.4) for 6 h. Following equilibration, the volume of the plasma and buffer samples removed from each equilibration cell was noted. Aliquots of dialyzed plasma (100 mL) and buffer (100 mL) were transferred to 96-well blocks, and acetonitrile (200 mL) containing indomethacin as internal standard (50 ng mL⁻¹) was added to each well. Each matrix was normalized to the other by the addition of equal volumes of the opposite matrix (i.e., plasma to buffer and buffer to plasma). Following extraction, the samples were then analyzed by LC/MS/MS.

Drug–Drug Interactions. The ability of a compound to act as a competitive inhibitor of the five major CYPs, namely, CYP1A2, 2C9, 2C19, 2D6, and 3A4, was examined as follows. Phenacetin (50 mM) (a probe substrate for CYP1A2), diclofenac (10 mM) (a probe substrate for CYP2C9), *S*-mephenytoin (50 mM) (a probe substrate for CYP2C19), bufuralol (10 mM) (a probe substrate for CYP2D6), testosterone (50 mM), or midazolam (5 mM) (probe substrates for CYP3A4) was incubated with human liver microsomes (CYP concentration = 0.25 mM), 3.3 mM MgCl₂, and 1.3 mM NADPH in a total volume of 0.6 mL of 100 mM phosphate buffer, pH 7.4, in the presence and absence of test compound at a concentration range of 0–50 mM. The reactions were initiated by the addition of NADPH, and incubations were conducted in a shaking water bath at 37 °C for 10 min, in the case of diclofenac, bufuralol, testosterone, and midazolam, or at 30 min, in the case of phenacetin and *S*-mephenytoin. All reactions were terminated by the addition of acetonitrile (200 mL), and the samples were centrifuged at 2500g for 5 min before LC/MS/MS analysis. Procedures for the quantitation of metabolites of probe P450 substrates used in the present study have been described in detail by Obach.⁴¹ Specific CYP enzyme inhibitors, ketoconazole (CYP3A4), quinidine (CYP2D6), sulfaphenazole (CYP2C9), (+)-*N*-3-benzylrivanol (CYP2C19), and furafylline (CYP1A2), were used as positive controls in the competitive inhibition studies.

Caco-2 Cell Permeability.⁴² Caco-2 cells, obtained from the American Type Culture Collection (Rockville, MD), were seeded in 24-well Falcon multiwell plates (polyethylene terephthalate membranes, pore size 1.0 mm) at 4.0×10^4 cells per well. The cells were grown on filter supports for 3 weeks. Permeability studies were performed after 15–17 days of culture. Cells were

used between passages 34 and 41. Complete culture medium was removed from both the apical and basolateral compartments, and the monolayer was preincubated with prewarmed apical (0.5 mL) or basolateral (1.5 mL) buffer for 0.5 h at 37 °C in a shaking water bath. The apical buffer consisted of Hank's balanced salt solution, 25 mM *D*-glucose monohydrate, 20 mM 2-(*N*-morpholino)ethanesulfonic acid, 1.25 mM CaCl₂, and 0.5 mM MgCl₂ (pH = 6.5). The basolateral buffer consisted of Hank's balanced salt solution, 25 mM *D*-glucose monohydrate, 20 mM *N*-(2-hydroxyethyl)piperazine-*N'*-2-ethanesulfonic acid, 1.25 mM CaCl₂, and 0.5 mM MgCl₂ (pH = 7.4). At the end of the preincubation, the media were removed and one (at concentrations of 1, 10, and 50 mM) or blank buffer was added. The effects of P-glycoprotein inhibitors on transport of **1** (1 mM) in both apical to basolateral (A to B) and basolateral to apical (B to A) directions were assessed by inclusion of verapamil (100 mM) or CP-100,356 (10 mM) in both donor and acceptor well solutions. To assess the integrity of the monolayer, the flux of [¹⁴C]mannitol from apical to basolateral was determined following incubation with **1**. Inserts with a flux greater than 2%/h were excluded from the study. Flux rate (F , mass/time) was calculated from the slope of the appearance of **1** on the receiver side, and the apparent permeability (P_{app}) was calculated from the equation $P_{app} \text{ (cm/s)} = (FV_D)/(SC_0)$, where S is surface area of the monolayer (0.83 cm²), V_D is the donor volume, and C_0 is the initial concentration in the donor compartment. Incubations were conducted in duplicate. Following extraction, the samples were then analyzed by LC/MS/MS.

In Vivo Pharmacokinetic Studies. The Pfizer Institutional Animal Care and Use Committee approved all procedures. Male and female Sprague-Dawley rats (220–250 g), beagle dogs (9–13 kg), and cynomolgus monkeys (4–6 kg) were used for these studies. All animals were fasted overnight before dosing. **1** was administered via the jugular vein (rats) or via the brachial vein (dogs and monkeys). **1** was administered iv at 3 mg/kg and orally (po) at 10, 30, and 100 mg/kg in rats (administered in 20% cremophor/10% ethanol/70% water), 3 mg/kg iv and 5 mg/kg po in monkeys (administered in glycerol formal), and 3 mg/kg iv and 5 mg/kg po in dogs (administered in glycerol formal). For all po studies, **1** was given as a suspension in 0.5% methylcellulose. Blood samples were taken, via the jugular vein (rats and dogs) or femoral vein (monkeys), in series at appropriate time intervals, and urine samples were also collected from rats for the length of the entire study (0–24 h). All samples were kept frozen until analysis. Following extraction, the samples were then analyzed by LC/MS/MS.

Compound Preparation and Characterization. Routine ¹H nuclear magnetic resonance (NMR) and ¹³C NMR spectra were recorded on a Varian Inova 400 MHz spectrometer unless otherwise specified. NMR structure elucidation experiments were collected using a Bruker DMX-500 spectrometer equipped with a Bruker 5 mm broad-band observe (BBO) probe at 300 K. Standard pulse sequences and phase cycling were used for all correlation spectroscopy (COSY), heteronuclear single-quantum coherence (HSQC), heteronuclear multiple bond coherence (HMBC), and nuclear Overhauser enhancement spectroscopy (NOESY) spectra. Low-resolution mass spectral data were collected using a Waters Micromass ZMD (electrospray ionization, chromatography on a Varian Polaris 5 C-18 column with acetonitrile and 0.1% formic acid aqueous gradient eluant). Compounds were determined to be $\geq 95\%$ pure by HPLC [C18, 0% acetonitrile in water (0.1% trifluoroacetic acid) to 60% acetonitrile, UV 220 nm]. Reagents and solvents were obtained from commercial sources unless otherwise noted. All reactions were run under nitrogen unless otherwise noted. Chiral separations were conducted using a Voyager instrument with a Chiralpak AD column and a mobile phase of ethanol/hexane or isopropanol/hexane. X-ray data were collected at 1 Å (maximum sin $\Theta/\lambda = 0.5$) on a Siemens R4RA/v diffractometer at room temperature.

Compound Synthesis. 3-((3*R*,4*R*)-4-Methyl-3-(methyl(7*H*-pyrrolo[2,3-*d*]pyrimidin-4-yl)amino)piperidin-1-yl)-3-oxopropanenitrile (1) Monocitrate. A mixture of 4-chloro-7*H*-pyrrolo[2,3-*d*]pyrimidine (5) (2.4 g, 15.9 mmol), prepared by the method of Davoll,⁴³ (3*R*,4*R*)-1-benzyl-*N*,4-dimethylpiperidin-3-amine (1.7 g, 7.95 mmol), prepared by the method of Brown Ripin²¹ and resolved as described in WO 02/096909, and 10 mL of triethylamine was heated in a sealed tube at 100 °C for 4 days. After cooling to room temperature and concentration under reduced pressure, the residue was purified by flash chromatography (silica; 3% methanol in dichloromethane) affording 1.0 g (38%) of (3*R*,4*R*)-1-benzyl-4-methylpiperidin-3-yl)methyl(7*H*-pyrrolo[2,3-*d*]pyrimidin-4-yl)-amine (19a) as a colorless oil. Alternative coupling conditions can be found in WO 02/096909. Low-resolution mass spectrometry (LMRS): m/z 336.1 (MH⁺). ¹H NMR (400 MHz) (CDCl₃) δ : 0.95 (3 H, d, J = 6.8 Hz), 1.61–1.75 (1 H, m), 1.81 (1 H, br s), 2.37 (2 H, br s), 2.82–2.95 (1 H, m), 3.54 (2 H, s), 3.61 (3 H, s), 5.21 (1 H, br s), 6.58 (1 H, d, J = 4.0 Hz), 7.18–7.40 (5 H, m), 8.25 (1 H, s). Alternatively, compound 19 was prepared by coupling racemic 1-benzyl-*N*,4-dimethylpiperidin-3-amine with 5. Compound 19 was then separated by chiral HPLC (Chiralpak AD; 85:15 hexanes/ethanol); 19a had a retention time of 7.43 min, and 19b had a retention time of 6.90 min. Compound 1 was then prepared from 19a, and compound 1a was prepared from 19b as described below.

To a solution of 79 g of (3*R*,4*R*)-1-benzyl-4-methylpiperidin-3-yl)methyl(7*H*-pyrrolo[2,3-*d*]pyrimidin-4-yl)amine dissolved in 2 L of ethanol was added 79 g of 20% palladium hydroxide on carbon (50% water by weight), and the mixture was agitated under an atmospheric pressure of 50 psi hydrogen for 3 days [conducting the hydrogenolysis at elevated temperature (50–70 °C) significantly decreases reaction times]. After the catalyst was removed by filtration through Celite, 51 g of cyanoacetic acid 2,5-dioxypyrrolidin-1-yl ester was added to the ethanolic solution, and the resulting mixture was stirred at room temperature for 1 h, at which time the ethanol was removed under reduced pressure. The residue was redissolved in 1.0 L of dichloromethane, and the solution was sequentially washed with 0.6 L of saturated aqueous sodium bicarbonate and 0.4 L of saturated sodium bicarbonate. The combined aqueous layers were back-washed with 0.4 L of 30 dichloromethane, and the dichloromethane layers were combined, dried over magnesium sulfate, filtered, and concentrated *in vacuo* affording 61 g of amber oil. This material was then redissolved in 2.1 L of acetone, and the solution was heated to 40 °C. Finely ground citric acid (37 g) was added slowly (as a solid) to the solution. The mixture continued stirring at 40 °C for 2 h (granulation was complete). After being cooled to room temperature, the solids were collected by filtration, washed with acetone, and dried *in vacuo* affording 78.5 g of 3-((3*R*,4*R*)-4-methyl-3-(methyl(7*H*-pyrrolo[2,3-*d*]pyrimidin-4-yl)amino)piperidin-1-yl)-3-oxopropanenitrile monocitrate (1 monocitrate) (66% from (3*R*,4*R*)-1-benzyl-4-methylpiperidin-3-yl)methyl(7*H*-pyrrolo[2,3-*d*]pyrimidin-4-yl)amine) as a slightly off-white crystalline solid. This material was then combined with 750 mL of 1:1 v/v ethanol/water, and the slurry was agitated overnight. The solids were filtered and dried to afford 69 g of 1 monocitrate as a white crystalline solid (mp = 201 dec). LRMS: m/z 313.2 (MH⁺). ¹H NMR (400 MHz) (D₂O) δ HOD: 0.92 (2 H, d, J = 7.2 Hz), 0.96 (1 H, d, J = 7.6 Hz), 1.66 (1 H, m), 1.80 (1 H, m), 2.37 (1 H, m), 2.58 (2 H, 1/2 ABq, J = 15.4 Hz), 2.70 (2 H, 1/2 ABq, J = 15.4 Hz), 3.23 (2 H, s), 3.25 (1 H, s), 3.33 (1 H, m), 3.46 (1 H, m), 3.81 (4 H, m), 4.55 (1 H, m), 6.65 (1 H, d, J = 3.2 Hz), 7.20 (1 H, t, J = 3.2 Hz), 8.09 (1 H, m). Anal. Calcd for C₂₂H₂₈N₆O₈: C, 52.38; H, 5.59; N, 16.66. Found: C, 52.32; H, 5.83; N, 16.30. For additional characterization of the monocitrate salt of 1 see WO 03/048162.

9-(7*H*-Pyrrolo[2,3-*d*]pyrimidin-4-yl)-2,3,4,4a,9,9a-hexahydro-1*H*-carbazole (2a). To a stirred solution of 5 (2 g/0.013 mol) in 100 mL of dimethylformamide was added 3.3 g (0.013 mol) of 2,3,4,4a,9,9a-hexahydro-1*H*-carbazole hydrobromide followed by 2.1 mL of pyridine, and the resulting mixture was stirred at

reflux for 16 h. After being cooled to room temperature the reaction mixture was washed with 10% CuSO₄ and saturated brine and dried over MgSO₄. Following filtration and concentration under reduced pressure the crude product (3.42 g) was purified by column chromatography (silica gel; 1:1 ethyl acetate/hexanes) affording 1.06 g (28%) of 2a as an off-white solid. LRMS: m/z 291 (MH⁺). ¹H NMR (400 MHz) (CDCl₃) δ : 1.21–1.45 (3 H, m), 1.67 (4 H, br s), 1.81–1.99 (1 H, m), 2.33 (2 H, dd, J = 32.0 Hz, J = 11.6 Hz), 3.62 (1 H, s), 4.86 (1 H, br s), 7.00–7.18 (2 H, m), 7.19–7.35 (3 H, m), 8.35 (1 H, d, J = 6.8 Hz). High-resolution mass spectrometry (HRMS): calcd for C₁₈H₁₈N₄ (MH⁺) 291.1604, found 291.1613.

4-(Piperidin-1-yl)-7*H*-pyrrolo[2,3-*d*]pyrimidine (2b). To a stirred solution of 5 (0.5 g/3.3 mmol) dissolved in 5 mL of *tert*-butanol was added 1.1 g (13 mmol) of piperidine, and the resulting mixture was heated to 85 °C for 3 h. After being cooled to room temperature the pH of the reaction mixture was adjusted to ~1 with 1 N HCl (aqueous) and washed 2 × 20 mL with ether. The aqueous layer was then basified with 1 N NaOH precipitating the product, which was collected by filtration and dried in a desiccator affording 395 mg (60%) of 2b as a white solid. LRMS: m/z 203.1. ¹H NMR (400 MHz) (CDCl₃) δ : 1.69 (6 H, s), 3.88 (4 H, s), 6.47 (1 H, d, J = 3.2 Hz), 7.06 (1 H, d, J = 3.2 Hz), 8.32 (1 H, s), 11.65 (1 H, br s). ¹³C NMR (400 MHz) (CDCl₃) δ : 24.8, 25.9, 47.3, 101.5, 102.9, 120.3, 150.9, 152.2, 157.3. HRMS: calcd for C₁₁H₁₅N₄ (MH⁺) 203.1291, found 203.1296.

Compounds 2c through 2i were prepared in an analogous manner to that described for 2b.

4-(2,5-Dimethylpyrrolidin-1-yl)-7*H*-pyrrolo[2,3-*d*]pyrimidine (2c). LRMS: m/z 217.3 (MH⁺). ¹H NMR (400 MHz) (CD₃OD) δ : 1.43 (6 H, d, J = 6.3 Hz), 1.82–1.87 (2 H, m), 2.14–2.17 (2 H, m), 4.50–4.53 (2 H, m), 6.55 (1 H, d, J = 3.5 Hz), 7.07 (1 H, d, J = 3.5 Hz), 8.07 (1 H, s). ¹³C NMR (400 MHz) (CD₃OD) δ : 21.2, 31.4, 55.1, 101.7, 102.5, 120.5, 150.2, 150.7, 155.0.

4-(Octahydro-1*H*-indol-1-yl)-7*H*-pyrrolo[2,3-*d*]pyrimidine (2d). LRMS: m/z 243.3 (MH⁺). ¹H NMR (400 MHz) (CDCl₃) δ : 1.18–1.43 (3 H, m), 1.55 (1 H, d, J = 10.8 Hz), 1.62–1.95 (4 H, m), 2.16 (1 H, s), 2.26 (1 H, br s), 2.40 (1 H, br s), 3.82 (1 H, d, J = 7.6 Hz), 3.95 (1 H, d, J = 8.8 Hz), 4.38 (1 H, br s), 6.50 (1 H, s), 7.04 (1 H, s), 8.30 (1 H, s).

***N*-Cyclopentyl-*N*-methyl-7*H*-pyrrolo[2,3-*d*]pyrimidin-4-amine (2e).** LRMS: m/z 217.2 (MH⁺). ¹H NMR (400 MHz) (CDCl₃) δ : 1.58–2.05 (9 H, m), 3.22 (3 H, s), 5.31 (1 H, t, J = 7.6 Hz), 6.56 (1 H, d, J = 3.6 Hz), 7.02 (1 H, d, J = 3.6 Hz), 8.29 (1 H, s).

***N*-Cyclohexyl-*N*-methyl-7*H*-pyrrolo[2,3-*d*]pyrimidin-4-amine (2f).** LRMS: m/z 231.2 (MH⁺). ¹H NMR (400 MHz) (CDCl₃) δ : 1.07–1.28 (2 H, m), 1.39–1.62 (3 H, m), 1.73 (2 H, d, J = 13.6 Hz), 1.78–1.95 (4 H, m), 3.22 (3 H, s), 4.68 (1 H, br s), 6.53 (1 H, d, J = 3.2 Hz), 7.02 (1 H, d, J = 3.6 Hz), 8.30 (1 H, s). ¹³C NMR (400 MHz) (CDCl₃) δ : 25.7, 25.9, 29.7, 30.4, 30.9, 55.4, 102.0, 102.8, 119.8, 150.9, 151.8, 157.5. HRMS: calcd for C₁₃H₁₉N₄ (MH⁺) 231.1604, found 231.1603.

***N*-Methyl-*N*-(4-methylcyclohexyl)-7*H*-pyrrolo[2,3-*d*]pyrimidin-4-amine (2g).** LRMS: m/z 245.2 (MH⁺). ¹H NMR (400 MHz) (CDCl₃) δ : 0.91 (1.5 H, d, J = 6.4 Hz), 1.02 (1.5 H, d, J = 7.2 Hz), 1.17 (2 H, q, J = 10.0 Hz), 1.38 (2 H, br s), 1.60 (3 H, t, J = 14.0 Hz), 1.70–2.03 (3 H, m), 3.20 (1.5 H, s), 3.24 (1.5 H, s), 4.64 (1 H, br s), 6.51 (1 H, t, J = 3.2 Hz), 7.03 (1 H, d, J = 3.2 Hz), 8.27 (1 H, s).

***N*-Cycloheptyl-*N*-methyl-7*H*-pyrrolo[2,3-*d*]pyrimidin-4-amine (2h).** LRMS: m/z 245.5 (MH⁺). ¹H NMR (400 MHz) (CD₃OD) δ : 1.40–1.83 (12 H, m), 3.09 (3 H, s), 3.21 (1 H, s), 6.50 (1 H, d, J = 3.6 Hz), 6.96 (1 H, d, J = 3.2 Hz), 7.97 (1 H, s). ¹³C NMR (400 MHz) (CD₃OD) δ : 26.4, 28.8, 32.1, 33.4, 58.8, 103.3, 104.0, 121.5, 151.7, 151.9, 158.2. HRMS: calcd for C₁₄H₂₁N₄ (MH⁺) 245.1761, found 245.1759.

***N*-Cyclooctyl-*N*-methyl-7*H*-pyrrolo[2,3-*d*]pyrimidin-4-amine (2i).** LRMS: m/z 259.3 (MH⁺). ¹H NMR (400 MHz) (CDCl₃) δ : 1.46–1.85 (14 H, m), 3.19 (3 H, s), 5.03 (1 H, br s), 6.56 (1 H, d, J = 3.2 Hz), 7.00 (1 H, d, J = 3.2 Hz), 8.29 (1 H, s), 9.79 (1 H, br s).

HSA Protocol. Ketones (**3**) (1 mmol) were added to tarred 4 mL vials and dissolved in 2 mL of methanol containing 4 mmol of methylamine. Acetic acid (120 mg/2 mmol as a 4 M solution in dichloroethane) was added followed by 1 g of borohydride polymer support (Amberlite IRA-400, 2.5 mmol BH_4/g resin), and the capped vials were agitated for 18 h at room temperature. The reaction mixtures were then transferred to filters to remove the resin, the resin was washed 2×3 mL with methanol, and the samples were concentrated affording crude amines **4**, which were carried on without additional purification. To these vials was added **5** (0.5 mmol) as a 0.5 M solution in tetrahydrofuran (THF) followed by 3 mL of a 10% solution of dichloroethane in *tert*-butanol and 1 M in diisopropylethylamine. The resulting capped mixtures were agitated at 80 °C for 40 h and then concentrated in a vacuum oven at 35 °C. The crude products were dissolved in 3 mL of 10% methanol in dichloromethane and transferred to 6 cm^3 strong cation-exchange (SCX) columns that had been preconditioned with 3 column volumes of methanol. The columns were then washed 3×5 mL with methanol, and the product was eluted with 5 mL of 0.1 N ammonia affording test compounds **6** after drying in a vacuum oven at 35 °C. QC was performed on all final compounds by LRMS and HPLC [C18, 5 μm , 19×100 mm; solvent A, 0.1% trifluoroacetic acid in water (v/v); solvent B, 0.1% trifluoroacetic acid in acetonitrile (v/v)].

Preparation of **4a** through **4h** was conducted in an analogous manner to that described in the HSA Protocol starting with ketones **3a** through **3h**. Some amine intermediates (**4**) were carried on without characterization.

N,3-Dimethylcyclohexanamine (4a) (Formate). ^1H NMR (400 MHz) (CDCl_3) δ : 0.97 (3 H, d, $J = 7.2$ Hz), 1.23 (1 H, dd, $J = 11.6$ Hz, $J = 12.4$ Hz), 1.25 (1 H, br s), 1.52–1.73 (4 H, m), 1.78–1.91 (2 H, m), 1.98–2.15 (1 H, m), 2.59 (3 H, s), 3.12 (1 H, q, $J = 3.6$ Hz), 8.61 (1 H, br s). HRMS: calcd for $\text{C}_8\text{H}_{17}\text{N}$ (MH^+) 128.1434, found 128.1433.

N,2-Dimethylcyclohexanamine (4b) (Formate). ^1H NMR (400 MHz) (CDCl_3) δ : 0.89–1.08 (3 H, m), 1.22 (2 H, br s), 1.28–1.81 (5 H, m), 2.01 (1 H, br s), 2.23 (1 H, br s), 2.68 (3 H, s), 2.91 (1 H, d, $J = 9.2$ Hz), 8.47 (1 H, s). HRMS: calcd for $\text{C}_8\text{H}_{17}\text{N}$ (MH^+) 128.1434, found 128.1432.

N,2,5-Trimethylcyclohexanamine (4c) (Formate). ^1H NMR (400 MHz) (CDCl_3) δ TMS: 0.89 (3 H, d, $J = 6.0$ Hz), 0.94 (3 H, d, $J = 7.4$ Hz), 0.95–1.12 (2 H, m), 1.21–1.63 (3 H, m), 1.75 (1 H, dd, $J = 28.0$ Hz, $J = 12.4$ Hz), 2.74 (1 H, br s), 2.81 (3 H, s), 2.92 (1 H, d, $J = 10.8$ Hz), 8.46 (1 H, br s). HRMS: calcd for $\text{C}_9\text{H}_{19}\text{N}$ (MH^+) 142.1590, found 142.1590.

2-Isopropyl-N,5-dimethylcyclohexanamine (4f) (Formate). ^1H NMR (400 MHz) (CDCl_3) δ : 0.61–0.78 (9 H, m), 0.82 (1 H, d, $J = 6.4$ Hz), 0.91 (1 H, t, $J = 12.8$ Hz), 1.08–1.32 (1 H, m), 1.43–1.65 (2 H, m), 1.84 (1 H, d, $J = 14.8$ Hz), 2.41 (3 H, s), 3.14 (1 H, s), 8.32 (1 H, s). HRMS: calcd for $\text{C}_{11}\text{H}_{23}\text{N}$ (MH^+) 170.1903, found 170.1902.

N-Methyl-N-(3-methylcyclohexyl)-7H-pyrrolo[2,3-d]pyrimidin-4-amine (6a). To a slurry of **5** (50 mg/0.32 mmol) in 1 mL of *tert*-butanol was added 45 mg (0.35 mmol) of **4a** followed by 84 mg (0.65 mmol) of diisopropylethylamine, and the resulting mixture was heated to 80 °C for 24 h. The reaction mixture was then cooled to room temperature and diluted with 25 mL of dichloromethane. The solution was washed with 1 N HCl and then with saturated NaHCO_3 , dried over Na_2SO_4 , and concentrated to dryness *in vacuo*. The crude product was then purified by preparative thin-layer chromatography (TLC) (silica gel; 2:1 hexanes/ethyl acetate) affording 20 mg of **6a** (25%) as an ~2:1 mixture of diastereomers. LRMS: m/z 245.2 (MH^+). ^1H NMR (400 MHz) (CD_3OD) δ : 0.68–0.80 (1 H, m), 0.84 (1 H, d, $J = 7.2$ Hz), 1.03 (2 H, d, $J = 6.8$ Hz), 1.18 (1 H, q, $J = 12.2$ Hz), 1.31–1.68 (5 H, m), 1.69–1.82 (1 H, m), 2.08 (1 H, br s), 3.06 (2 H, s), 3.09 (1 H, s), 3.21 (1 H, s), 4.55 (1 H, br s), 6.46 (0.3 H, d, $J = 3.6$ Hz), 6.48 (0.7 H, d, $J = 2.0$ Hz), 6.97 (1 H, t, $J = 2.0$ Hz), 7.98 (0.3 H, s), 7.99 (0.7 H, s). ^{13}C NMR (400 MHz) (CD_3OD) δ : 21.1, 23.7,

25.5, 28.8, 32.2, 33.0, 33.9, 33.9, 34.2, 34.4, 36.2, 37.9, 42.3, 54.3, 59.2, 105.7, 105.8, 106.7, 124.1, 154.2, 154.2, 154.4, 161.2, 161.4. HRMS: calcd for $\text{C}_{14}\text{H}_{21}\text{N}_4$ (MH^+) 245.1761, found 245.1756.

Compounds **6b** through **6h** were prepared in an analogous manner to that described for **6a**. Compounds **6d**, **6e**, **6g**, and **6h** were characterized by LRMS and HPLC purity as described above.

N-Methyl-N-(2-methylcyclohexyl)-7H-pyrrolo[2,3-d]pyrimidin-4-amine (6b) (~3:1 Mixture of Diastereomers). LRMS: m/z 245.5 (MH^+). ^1H NMR (400 MHz) (CD_3OD) δ : 0.66 (0.75 H, d, $J = 7.0$ Hz), 0.92 (2.25 H, d, $J = 7.0$ Hz), 0.98–1.24 (1 H, m), 1.25–1.42 (2 H, m), 1.43–1.55 (2 H, m), 1.56–1.82 (2 H, m), 1.90 (1 H, sp q), 2.29 (1 H, br s), 3.15 (2.25 H, s), 3.21 (0.75 H, s), 4.52–4.60 (1 H, m), 6.48 (1 H, d, $J = 3.6$ Hz), 6.97 (1 H, d, $J = 3.2$ Hz), 7.98 (0.25 H, s), 8.00 (0.75 H, s). ^{13}C NMR (400 MHz) (CD_3OD) δ : 13.5, 19.4, 20.9, 26.3, 26.9, 27.0, 27.9, 33.5, 34.0, 34.1, 36.0, 36.4, 59.7, 103.4, 104.0, 121.6, 151.4, 151.7, 158.6, 159.4. HRMS: calcd for $\text{C}_{14}\text{H}_{21}\text{N}_4$ (MH^+) 245.1761, found 245.1754.

N-(2,5-Dimethylcyclohexyl)-N-methyl-7H-pyrrolo[2,3-d]pyrimidin-4-amine (6c) (Mixture of Diastereomers). LRMS: m/z 259.1 (MH^+). ^1H NMR (400 MHz) (CD_3OD) δ : 0.68 (1 H, d, $J = 6.8$ Hz), 0.82 (1 H, d, $J = 7.0$ Hz), 0.84 (2 H, d, $J = 6.0$ Hz), 0.88 (1 H, d, $J = 7.2$ Hz), 1.01–1.22 (1 H, m), 1.22–1.41 (1 H, m), 1.42–1.62 (2 H, m), 1.63–1.76 (1 H, m), 1.77–1.89 (0.5 H, m), 2.05 (0.5 H, d, $J = 12.2$), 2.15 (0.5 H, br s), 2.26 (0.5 H, br s), 3.02 (0.5 H, s), 3.08 (0.5 H, s), 3.14 (1.5 H, s), 3.18 (1.5 H, s), 4.55–4.62 (1 H, m), 6.42–6.54 (1 H, m), 6.92–6.99 (1 H, m), 7.96–8.07 (1 H, m). ^{13}C NMR (400 MHz) (CD_3OD) δ : 22.7, 23.0, 28.4, 29.0, 29.7, 29.8, 30.2, 31.1, 32.3, 33.0, 33.2, 33.6, 33.9, 34.0, 34.7, 34.8, 34.8, 35.4, 35.7, 35.8, 36.2, 36.9, 39.3, 48.4, 48.6, 48.8, 49.0, 49.2, 49.5, 49.7, 54.1, 59.4, 103.4, 104.1, 104.1, 121.5, 121.5, 151.6, 151.7, 151.8, 151.9, 152.0, 158.7, 159.2, 159.4. HRMS: calcd for $\text{C}_{15}\text{H}_{23}\text{N}_4$ (MH^+) 259.1917, found 259.1917.

N-(2-Isopropyl-5-methylcyclohexyl)-N-methyl-7H-pyrrolo[2,3-d]pyrimidin-4-amine (6f) (~3:1 Mixture of Diastereomers). LRMS: m/z 287.4 (MH^+). ^1H NMR (400 MHz) (CD_3OD) δ : 0.55 (1 H, br s), 0.71 (3 H, d, $J = 7.0$ Hz), 0.79 (1 H, d, $J = 7.0$ Hz), 0.91 (3 H, d, $J = 6.4$ Hz), 0.97 (3 H, d, $J = 4.0$ Hz), 1.38–1.60 (3 H, m), 1.61–1.73 (2 H, m), 1.82–2.00 (2 H, m), 3.21 (1 H, s), 3.21 (3 H, s), 4.62 (1 H, br s), 6.49 (0.75 H, d, $J = 2.8$ Hz), 6.55 (0.25 H, s), 6.99 (1 H, s), 7.99 (0.25 H, s), 8.01 (0.75 H, s). ^{13}C NMR (400 MHz) (CD_3OD) δ : 16.5, 21.5, 21.9, 22.7, 23.0, 24.9, 26.0, 28.1, 28.4, 31.8, 33.4, 34.1, 34.6, 35.6, 36.6, 39.4, 43.3, 46.1, 48.4, 48.6, 48.8, 49.0, 49.3, 49.7, 49.7, 60.9, 103.7, 104.0, 122.0, 150.4, 150.6, 150.9, 158.0. HRMS: calcd for $\text{C}_{17}\text{H}_{27}\text{N}_4$ (MH^+) 287.2230, found 287.2231.

(5S)-2-Methyl-5-(prop-1-en-2-yl)cyclohexanone (8). A solution of *S*-(+)-carvone (**7**) (2.05 g/13.6 mmol) dissolved in 14 mL of dry THF was cooled to -70 °C, and to this mixture was added dropwise 14 mL of a 1.0 M solution of *L*-selectride in THF. Once the addition was complete, the reaction mixture stirred at -70 °C for 2 h, at which time the reaction was warmed to 0 °C and 40 mL of a 10% solution of sodium hydroxide was added dropwise with stirring over a 10 min period. Hydrogen peroxide (30%, 28 mL) was then added dropwise over a 10 min period, and the mixture was warmed to room temperature, transferred to a separatory funnel, and extracted 3×100 mL with hexanes. The organic extracts were washed 2×100 mL with water, 2×100 mL with 1.5 M sodium bisulfite, and 50 mL with saturated brine. The organic layer was then dried over MgSO_4 , filtered through Celite, and concentrated to dryness *in vacuo*. The crude product was then purified by flash chromatography (silica gel; 95:5 hexanes/ethyl acetate) affording 1.08 g (52%) of compound **8** as a colorless oil. LRMS: m/z 153.4 (MH^+). ^1H NMR (400 MHz) (CDCl_3) δ : 1.00 (2.5 H, d, $J = 6.4$ Hz), 1.03 (0.5 H, d, $J = 6.8$ Hz), 1.30–1.38 (1 H, m), 1.60 (1 H, d, $J = 9.2$ Hz), 1.69 (3 H, s), 1.84 (1 H, d, $J = 25.6$ Hz), 2.05–2.12 (1 H, m), 2.98–2.43 (4 H, m), 4.69 (2 H, d, $J = 10.4$ Hz).

(5S)-N,2-Dimethyl-5-(prop-1-en-2-yl)cyclohexanamine (9). To a 250 mL round-bottom flask was charged 3.21 g (15.1 mmol) of

sodium triacetoxyborohydride and 1.08 g (7.1 mmol) of **8** dissolved in 70 mL of THF, to this mixture was added 3.6 mL of 2.0 M solution of methylamine in THF, and the resulting mixture was stirred at room temperature for 16 h, at which time the reaction was quenched upon addition of 75 mL of water. The resulting mixture was extracted 3 × 100 mL with chloroform, and the combined organic extracts were dried over MgSO₄, filtered through Celite, and concentrated to dryness *in vacuo*. The crude product was then purified by flash chromatography (silica gel; 6:4 dichloromethane/hexanes to 9:1 dichloromethane/methanol) affording **9** as a colorless oil. LRMS: *m/z* 168.5 (MH⁺). ¹H NMR (400 MHz) (CDCl₃) δ: 0.79 (2 H, d, *J* = 7.2 Hz), 0.87 (1 H, d, *J* = 6.8 Hz), 1.14 (1 H, t, *J* = 4.8 Hz), 1.21–1.55 (3 H, m), 1.56–1.73 (2 H, m), 1.65 (3 H, s), 1.80–2.20 (2 H, m), 2.34 (1 H, s), 2.35 (2 H, s), 2.47 (0.6 H, d, *J* = 12 Hz), 2.57 (0.3 H, d, *J* = 3.2 Hz), 4.61 (2 H, d, *J* = 3.6 Hz).

N-Methyl-N-((5S)-2-methyl-5-(prop-1-en-2-yl)cyclohexyl)-7H-pyrrolo[2,3-d]pyrimidin-4-amine (Diastereomeric Mixture 11). A sealed tube was charged with 119 mg (0.78 mmol) of **5**, 233 mg (1.02 mmol) of **9**, 320 mg (3.16 mmol) of triethylamine, and 3 mL of *tert*-butanol, and the capped mixture was stirred at 100 °C for 48 h. After being cooled to room temperature the mixture was diluted with 30 mL of ether, transferred to a separatory funnel, and washed 2 × 20 mL with 1 N HCl, and the aqueous layers were combined and adjusted to pH 12 with 2 N KOH. The resulting basic layer was extracted 3 × 100 mL with dichloromethane, and the combined dichloromethane extracts were dried over MgSO₄, filtered through Celite, and concentrated under reduced pressure affording a yellow oil. The crude product was then purified by flash chromatography (silica gel; 7:3 ethyl acetate/hexanes), and the fraction with an *R_f* = 0.16 was collected and concentrated to dryness *in vacuo* affording 10.4 mg of compound **11** as a white solid. LRMS: *m/z* 285.3 (MH⁺). ¹H NMR (400 MHz) (CDCl₃) δ: 0.82 (1.5 H, d, *J* = 6.4 Hz), 1.00 (1.5 H, d, *J* = 7.2 Hz), 1.40–1.48 (1 H, m), 0.65 (0.5 H, d, *J* = 13.2 Hz), 0.70 (0.5 H, d, *J* = 13.6 Hz), 1.69–1.95 (4 H, m), 1.72 (1.5 H, s), 1.75 (1.5 H, s), 2.05–2.22 (1 H, m), 2.45 (1 H, br s), 3.21 (1 H, s), 3.28 (3 H, s), 4.70 (1 H, d, *J* = 12.4 Hz), 4.73 (1 H, d, t, *J* = 2.8 Hz), 4.77 (1 H, br s), 6.51 (0.5 H, d, *J* = 3.2 Hz), 6.55 (0.5 H, s), 7.02 (0.5 H, d, *J* = 3.6 Hz), 7.03 (0.5 H, d, *J* = 3.6 Hz), 8.26 (0.5 H, s), 8.28 (0.5 H, s).

Diastereomeric mixture **10** was prepared in an analogous manner to that described for **11** beginning with *R*-(–)-carvone.

N-Methyl-N-((1S,2R,5S)-2-methyl-5-(prop-1-en-2-yl)cyclohexyl)-7H-pyrrolo[2,3-d]pyrimidin-4-amine (12). Compound **12** was isolated from diastereomeric mixture **11** by chiral HPLC (Chiralpak AD; 9:1 hexanes/isopropanol + 0.1% DEA modifier). The retention time for **12** was 8.26 min; its diastereomer came off at 13.26 min. The peaks were collected and concentrated to dryness *in vacuo*. Physical data for **12**: LRMS: *m/z* 285.5 (MH⁺). ¹H NMR (400 MHz) (CDCl₃) δ: 1.01 (3 H, d, *J* = 6.8 Hz), 1.42 (sp t, *J* = 9.2 Hz), 1.58 (1 H, br d, *J* = 12.8 Hz), 1.63–1.94 (4 H, m), 1.75 (3 H, s), 2.11 (1 H, t, *J* = 11.6 Hz), 2.45 (1 H, br s), 3.30 (3 H, s), 4.73 (2 H, s), 4.77 (1 H, br s), 6.53 (1 H, d, *J* = 3.6 Hz), 7.04 (1 H, d, *J* = 3.6 Hz), 8.27 (1 H, s). 1D and 2D NMR structural assignments for **12** were consistent with the all-*cis* relative stereochemistry around the cyclohexane ring.

N-Methyl-N-((1S,2R,5S)-2-methyl-5-(prop-1-en-2-yl)cyclohexyl)-7-(phenylsulfonyl)-7H-pyrrolo[2,3-d]pyrimidin-4-amine (13). To 5 mL of dimethylformamide (DMF) was added 217 mg (5.43 mmol) of sodium hydride and after cooling to 0 °C was added 1.02 g (3.59 mmol) of **12** dissolved in 5 mL of DMF dropwise over a 10-min period. After bubbling ceased, 685 μL of phenylsulfonyl chloride was added, and the mixture was brought to room temperature and stirred for 1.5 h, at which time the reaction was quenched upon addition of 10 mL of water. The resulting mixture was then extracted 3 × 10 mL with dichloromethane, and the combined extracts were washed 2 × with water and 2 × with saturated brine, dried over MgSO₄, filtered, and concentrated under reduced pressure producing 1.1 g of a yellow oil. The oil

was purified by flash chromatography (silica gel; 9:1 hexanes/ethyl acetate) affording 748 mg (50%) of **13** as a white solid. LRMS: *m/z* 425.3 (MH⁺). ¹H NMR (400 MHz) (CDCl₃) δ: 0.94 (3 H, d, *J* = 7.2 Hz), 1.39 (1 H, dd, *J* = 13.2 Hz, *J* = 3.6 Hz), 1.49–1.65 (2 H, m), 1.72 (3 H, s), 1.75–1.86 (2 H, m), 2.06 (1 H, t, *J* = 12.0 Hz), 2.33 (1 H, br s), 3.18 (3 H, s), 4.64 (1 H, br s), 4.71 (2 H, s), 6.58 (1 H, d, *J* = 3.6 Hz), 7.42 (1 H, d, *J* = 4.4 Hz), 7.47 (2 H, d, *J* = 8.0 Hz), 7.56 (1 H, t, *J* = 2.0 Hz), 8.15 (2 H, d, *J* = 8.8 Hz), 8.37 (1 H, s).

(R)-2-((1S,3S,4R)-4-Methyl-3-(methyl(7-(phenylsulfonyl)-7H-pyrrolo[2,3-d]pyrimidin-4-yl)amino)cyclohexyl)propan-1-ol (14). To a stirred solution of **13** (745 mg/1.76 mmol) in 5 mL of THF was added 7.0 mL (3.50 mmol) of 9-borabicyclo(3.3.1)nonane (9-BBN) (0.5 M in THF; Aldrich), and the resulting solution was heated to reflux for 18 h (reaction incomplete by TLC). Additional 9-BBN (7.0 mL) was added with continued refluxing for 2 h, at which time the reaction was cooled to room temperature, and water (10 mL) slowly added. The reaction mixture was partitioned between saturated NaHCO₃ and dichloromethane, and the organic layer was washed 2 × with water and with saturated brine, dried over MgSO₄ and concentrated under reduced pressure. The resulting crude oil was then purified by flash chromatography (silica gel; 1:1 hexanes/ethyl acetate) affording 428 mg (55%) of **14** as a white solid. LRMS: *m/z* 443.1 (MH⁺). ¹H NMR (400 MHz) (CDCl₃) δ: 0.85–0.97 (6 H, m), 1.20–1.29 (1 H, m), 1.47 (1 H, d, *J* = 16.4 Hz), 1.55–1.64 (4 H, m), 1.65–1.80 (1 H, m), 2.33 (1 H, br s), 3.19 (3 H, s), 3.44–3.56 (1 H, m), 3.58–3.63 (1 H, m), 4.59 (1 H, br s), 6.58 (1 H, d, *J* = 3.6 Hz), 7.43 (1 H, d, *J* = 4.0 Hz), 7.49 (2 H, d, *J* = 8.0 Hz), 7.57 (1 H, t, *J* = 2.0 Hz), 8.16 (2 H, d, *J* = 7.2 Hz), 8.38 (1 H, s).

(R)-2-((1S,3S,4R)-4-Methyl-3-(methyl(7H-pyrrolo[2,3-d]pyrimidin-4-yl)amino)cyclohexyl)propan-1-ol (16a). To a stirred solution of **14** (400 mg/0.90 mmol) in 10 mL of THF at room temperature was added ~10 mL of a solution made by dissolving sodium hydroxide pellets in methanol. The resulting mixture was stirred until the reaction was complete by TLC (~3 h). To the reaction was then added 50 mL of water, and the mixture was extracted 3 × with ethyl acetate. The combined extracts were washed 2 × with water and saturated brine, dried over MgSO₄, filtered, and concentrated to dryness *in vacuo*, affording 196 mg (72%) of **16a** as a white solid. This material could also be prepared by direct hydroboration of compound **12** using 9-BBN. LRMS: *m/z* 303.5 (MH⁺). ¹H NMR (400 MHz) (CDCl₃) δ: 0.81 (1.5 H, d, *J* = 6.4 Hz), 0.86–1.00 (4.5 H, m), 1.14–1.26 (1 H, m), 1.37–2.49 (5 H, m), 1.55–2.64 (5 H, m), 3.21 (1 H, br s), 3.44–3.59 (1 H, m), 3.60–3.63 (1 H, m), 4.70 (1 H, br s), 6.48 (1 H, d, *J* = 3.6 Hz), 6.56 (1 H, br s), 7.00 (1 H, d, *J* = 3.6 Hz), 8.22 (0.5 H, s), 8.44 (0.5 H, s).

N,N-Diethyl-2-((R)-2-((1S,3S,4R)-4-methyl-3-(methyl(7H-pyrrolo[2,3-d]pyrimidin-4-yl)amino)cyclohexyl)propoxy)acetamide (16b). To a slurry of sodium hydride (7.0 mg, 60% dispersion) in 0.5 mL of DMF at 0 °C was added 49 mg (0.112 mmol) of **14** dissolved in 0.5 mL of DMF, the resulting mixture stirred at 0 °C for 30 min, at which time 15 μL (0.113 mmol) of 2-chloro-*N,N*-diethylacetamide (Aldrich) was added, and the resulting solution was stirred at 0 °C for 4 h, at which time 10 mL of water was added. This mixture was then extracted 3 × 15 mL with ethyl acetate, and the combined extracts were washed with 10 mL of water and then 10 mL of saturated brine, dried over MgSO₄, filtered, and concentrated under reduced pressure affording 45 mg of intermediate **15b**. This material (**15b**) was then dissolved in 1.0 mL of THF, and to this solution was added 1.0 mL of a solution made by dissolving NaOH pellets in methanol. The resulting mixture was stirred until the reaction was complete by TLC (~30 min). To the reaction was then added 10 mL of water, and the mixture was extracted 3 × with ethyl acetate. The combined extracts were washed 2 × with water and saturated brine, dried over MgSO₄, filtered, and concentrated to dryness *in vacuo*, affording 20 mg (61%) of **16b** as a colorless oil. LRMS: *m/z* 416.4 (MH⁺). ¹H NMR (400 MHz) (CDCl₃) δ: 0.78–0.92

(1 H, m), 0.93–0.96 (1 H, m), 0.97 (3 H, d, $J = 7.6$ Hz), 1.10 (3 H, t, $J = 7.2$ Hz), 1.16–1.20 (3 H, m), 1.24 (1 H, s), 1.43 (2 H, br s), 1.52–1.63 (4 H, m), 1.75 (2 H, q, $J = 4.0$ Hz), 3.15–2.28 (1 H, m), 3.30 (3 H, s), 3.31 (2 H, s), 3.32–3.43 (2 H, m), 4.69 (2 H, br s), 5.01 (4 H, q, $J = 11.6$ Hz), 6.52 (1 H, d, $J = 3.6$ Hz), 7.01 (1 H, d, $J = 3.6$ Hz), 8.27 (1 H, s).

***N*-Methyl-2-((*R*)-2-((1*S*,3*S*,4*R*)-4-methyl-3-(methyl(7*H*-pyrrolo[2,3-*d*]pyrimidin-4-yl)amino)cyclohexyl)propoxy)acetamide (16c).** LRMS: m/z 374.1 (MH^+). 1H NMR (400 MHz) ($CDCl_3$) δ : 0.78–1.03 (6 H, m), 1.18–1.84 (9 H, m), 3.27 (1.5 H, s), 3.32 (1.5 H, s), 3.49–3.59 (1 H, m), 3.60–3.69 (1 H, m), 3.91–4.06 (1 H, m), 4.21 (1 H, q, $J = 4.0$ Hz), 4.72 (1 H, br s), 6.45 (1 H, br s), 6.47 (0.5 H, d, $J = 12.0$ Hz), 6.52 (0.5 H, d, $J = 2.8$ Hz), 6.92 (0.5 H, d, $J = 3.6$ Hz), 6.99 (0.5 H, d, $J = 3.6$ Hz), 8.23 (0.5 H, s), 8.31 (0.5 H, s).

***N*-Benzyl-2-((*R*)-2-((1*S*,3*S*,4*R*)-4-methyl-3-(methyl(7*H*-pyrrolo[2,3-*d*]pyrimidin-4-yl)amino)cyclohexyl)propoxy)acetamide (16d).** LRMS: m/z 450.1 (MH^+). 1H NMR (400 MHz) ($CDCl_3$) δ : 0.78–1.03 (6 H, m), 1.37–1.82 (6 H, m), 2.41 (2 H, br s), 3.23 (3 H, s), 3.26 (1 H, s), 3.29 (1 H, s), 3.44–3.53 (1 H, m), 3.59–3.68 (1 H, m), 4.20 (1 H, q, $J = 7.2$ Hz), 4.37 (1 H, d, $J = 6.4$ Hz), 4.45 (1 H, dd, $J = 6.4$ Hz, $J = 4.4$ Hz), 4.71 (2 H, d, $J = 5.2$ Hz), 6.44 (1 H, br s), 6.55 (1 H, d, $J = 3.6$ Hz), 6.95 (1 H, d, $J = 3.6$ Hz), 7.19–7.35 (5 H, m), 8.24 (1 H, s).

(*R*)-2-((1*S*,3*S*,4*R*)-4-Methyl-3-(methyl(7*H*-pyrrolo[2,3-*d*]pyrimidin-4-yl)amino)cyclohexyl)propyl Diethylcarbamate (16e). LRMS: m/z 402.5 (MH^+). 1H NMR (400 MHz) ($CDCl_3$) δ : 0.72–1.00 (6 H, m), 1.18 (1 H, t, $J = 1.2$ Hz), 1.22 (3 H, s), 1.23 (3 H, s), 1.39–1.82 (6 H, m), 3.18–3.35 (7 H, m), 3.43–3.66 (1 H, m), 3.87–4.03 (1 H, m), 4.14 (1 H, dd, $J = 5.6$ Hz, $J = 25$ Hz), 0.67 (1 H, br s), 6.44 (1 H, br s), 6.82 (1 H, t, $J = 4.4$ Hz), 6.97 (1 H, d, $J = 3.6$ Hz), 8.25 (1 H, t, $J = 6.2$ Hz).

***cis*-*N*-Methyl-*N*-(4-methyl-1-(2,2,2-trifluoroethylsulfonyl)-piperidin-3-yl)-7*H*-pyrrolo[2,3-*d*]pyrimidin-4-amine (17a).** Compound **19** was deprotected as described above; however, the intermediate hydrogenolysis product *cis*-*N*-methyl-*N*-(4-methylpiperidin-3-yl)-7*H*-pyrrolo[2,3-*d*]pyrimidin-4-amine was isolated by filtration through Celite and concentration under reduced pressure. LRMS: m/z 246.0 (MH^+). 1H NMR (400 MHz) (CD_3OD) δ : 1.00–1.13 (5 H, m), 1.80 (1 H, br s), 1.95 (1 H, br s), 2.43 (1 H, br s), 3.07–3.18 (1 H, m), 3.38 (1 H, dd, $J = 7.6$ Hz, $J = 4.8$ Hz), 3.41 (3 H, s), 3.52 (1 H, q, $J = 7.2$ Hz), 3.61 (1 H, q, $J = 8.8$ Hz), 6.74 (1 H, br s), 7.11 (1 H, d, $J = 3.2$ Hz), 8.35 (1 H, br s). ^{13}C NMR (400 MHz) (CD_3OD) δ : 14.2, 29.4, 32.3, 38.5, 41.7, 43.9, 57.4, 104.3, 104.6, 123.2, 148.9, 149.5, 158.1. HRMS: calcd for $C_{13}H_{20}N_5$ (MH^+) 246.1713, found 246.1715. To this material (30 mg/0.122 mmol) dissolved in 1.0 mL of dichloromethane containing 0.1 mL of pyridine was added 20 μ L (0.181 mmol) of 2,2,2-trifluoroethanesulfonyl chloride, and the resulting mixture was stirred at room temperature for 16 h. The reaction mixture was then partitioned between dichloromethane and saturated sodium bicarbonate, the aqueous layer was back-washed 2 \times with dichloromethane, and the combined organic layers dried over sodium sulfate and concentrated to dryness *in vacuo*. The crude product was then purified by preparative TLC (silica gel; 20:1 dichloromethane/methanol) affording 9 mg (19%) of **17a** as a white powder. LRMS: m/z 392.1 (MH^+). 1H NMR (400 MHz) ($CDCl_3$) δ : 1.03 (3 H, d, $J = 6.8$ Hz), 1.78–1.96 (2 H, m), 2.35 (1 H, br s), 3.55 (1 H, dd, $J = 14.8$ Hz, $J = 4.0$ Hz), 3.58 (3 H, s), 3.61–3.75 (1 H, s), 3.75 (2 H, q, $J = 9.6$ Hz), 3.83 (1 H, dd, $J = 8.2$ Hz, $J = 5.6$ Hz), 5.39 (1 H, d, $J = 4.0$ Hz), 6.61 (1 H, d, $J = 3.2$ Hz), 7.11 (1 H, d, $J = 3.6$ Hz), 8.23 (1 H, s). ^{13}C NMR (400 MHz) ($CDCl_3$) δ : 15.2, 30.8, 32.0, 35.9, 43.9, 47.1, 52.4, 52.5, 103.3, 120.3, 121.6, 123.1, 145.8, 158.2. HRMS: calcd for $C_{15}H_{21}F_3N_5O_2S$ (MH^+) 392.1363, found 392.1369.

***cis*-4-Methyl-3-(methyl(7*H*-pyrrolo[2,3-*d*]pyrimidin-4-yl)amino)-*N*-(3-methylisothiazol-5-yl)piperidine-1-carboxamide (17b).** To a stirred solution of 3-methylisoxazol-5-amine (100 mg/1.00 mmol) in 2 mL of acetonitrile was added 103 mg (0.66 mmol) of phenylchloroformate, and the resulting mixture was stirred at

room temperature for 18 h. The reaction mixture was then diluted with dichloromethane, washed with saturated $NaHCO_3$, dried over $MgSO_4$, filtered, and concentrated to dryness *in vacuo*. The intermediate phenyl (3-methylisoxazol-5-yl)carbamate was carried on without further purification by forming a slurry in *tert*-butanol (2 mL) and adding 50 mg (0.20 mmol) of *cis*-*N*-methyl-*N*-(4-methylpiperidin-3-yl)-7*H*-pyrrolo[2,3-*d*]pyrimidin-4-amine; the resulting reaction mixture was heated to 80 $^{\circ}C$ for 48 h. After being cooled to room temperature the reaction was concentrated under reduced pressure, redissolved in dichloromethane, washed with saturated $NaHCO_3$, dried over $MgSO_4$, filtered through Celite, and concentrated to dryness *in vacuo*. The crude product was then purified by preparative TLC (silica gel; 10:1 dichloromethane/methanol) affording 7 mg of pure **17b** after two chromatographies. LRMS: m/z 386.2 (MH^+). 1H NMR (400 MHz) (CD_3OD) δ : 1.12 (3 H, d, $J = 7.2$ Hz), 1.70–2.00 (4 H, m), 2.30 (3 H, s), 2.45–2.56 (1 H, m), 3.44 (3 H, s), 3.67 (2 H, t, $J = 6.0$ Hz), 3.88–4.02 (1 H, m), 4.94 (1 H, br s), 6.62 (1 H, s), 6.71 (1 H, d, $J = 3.6$ Hz), 7.16 (1 H, d, $J = 3.6$ Hz), 8.15 (1 H, s). ^{13}C NMR (400 MHz) (CD_3OD) δ : 14.7, 18.8, 32.0, 33.3, 35.6, 42.6, 45.6, 104.0, 104.2, 107.7, 122.6, 155.8, 164.7, 164.9. HRMS: calcd for $C_{18}H_{24}N_7OS$ 386.1758 (MH^+), found 386.1751.

***cis*-*N*-(1-(2,3-Difluorobenzyl)-4-methylpiperidin-3-yl)-*N*-methyl-7*H*-pyrrolo[2,3-*d*]pyrimidin-4-amine (17c).** To a stirred solution of *cis*-*N*-methyl-*N*-(4-methylpiperidin-3-yl)-7*H*-pyrrolo[2,3-*d*]pyrimidin-4-amine (50 mg/0.20 mmol) and 156 μ L (1.43 mmol) of 2,3-difluorobenzaldehyde in 3 mL of anhydrous methanol was added 20 mg (0.31 mmol) of sodium cyanoborohydride, and the resulting mixture was stirred at room temperature for 3 h, at which time a second portion of sodium cyanoborohydride was added, and the resulting mixture was stirred for 72 h. The reaction was quenched upon addition of 2 drops of 1 N NaOH, and the reaction was concentrated under reduced pressure. Water was added, the mixture was extracted 3 \times with chloroform, and the combined chloroform extracts were dried over $MgSO_4$, filtered through Celite, and concentrated to dryness *in vacuo*. The crude product was then purified by flash chromatography (silica gel; 4% methanol in chloroform) affording 24 mg (32%) of **17c** as a white solid. LRMS: m/z 372.3 (MH^+). 1H NMR (400 MHz) ($CDCl_3$) δ : 0.93 (3 H, d, $J = 7.2$ Hz), 1.60–1.85 (4 H, m), 2.30 (1 H, br s), 2.62–2.83 (2 H, m), 2.87–2.96 (1 H, m), 3.59 (2 H, s), 3.61 (3 H, s), 5.22 (1 H, br s), 6.58 (1 H, d, $J = 4.0$ Hz), 6.95–7.08 (3 H, m), 7.13 (1 H, t, $J = 5.2$ Hz), 8.22 (1 H, s). HRMS: calcd for $C_{20}H_{24}N_5F_2$ (MH^+) 372.1994, found 372.1985.

***cis*-2-Hydroxy-1-(4-methyl-3-(methyl(7*H*-pyrrolo[2,3-*d*]pyrimidin-4-yl)amino)piperidin-1-yl)ethanone (17d).** To a stirred solution of *cis*-*N*-methyl-*N*-(4-methylpiperidin-3-yl)-7*H*-pyrrolo[2,3-*d*]pyrimidin-4-amine (200 mg/0.82 mmol) and 163 mg (0.98 mmol) of 2-(benzyloxy)acetic acid in 10 mL of dichloromethane at 0 $^{\circ}C$ was added 188 mg (0.98 mmol) of 1-ethyl-3-(3-dimethylaminopropyl)carbodiimide followed by 26 mg (0.21 mmol) of 4-dimethylaminopyridine, and the resulting mixture was brought to room temperature and stirred for 24 h, at which time the reaction mixture was partitioned between dichloromethane and saturated $NaHCO_3$. The dichloromethane layer was dried over $MgSO_4$, filtered through Celite, and concentrated to dryness *in vacuo* affording crude 2-(benzyloxy)-1-(4-methyl-3-(methyl(7*H*-pyrrolo[2,3-*d*]pyrimidin-4-yl)amino)piperidin-1-yl)ethanone, which was purified by flash chromatography (silica gel; 4% methanol in dichloromethane) affording 170 mg (53%) of this pure intermediate. LRMS: m/z 394.2 (MH^+). 1H NMR (400 MHz) (CD_3OD) (amide rotamers) δ : 1.06 (1.5 H, d, $J = 7.2$ Hz), 1.09 (1.5 H, d, $J = 7.2$ Hz), 1.61–1.74 (1 H, m), 1.80–1.91 (1 H, m), 2.40–2.52 (1 H, m), 3.31 (1.5 H, s), 3.35 (1.5 H, s), 3.37–6.64 (1 H, m), 3.72–3.99 (2 H, m), 4.09 (0.5 H, 1/2 AB q, $J = 12.8$ Hz), 4.25 (0.5 H, 1/2 AB q, $J = 13.2$ Hz), 4.27 (2 H, s), 4.27 (1 H, d, $J = 4.8$ Hz), 4.59 (2 H, s), 4.83–5.03 (1 H, m), 6.56 (0.5 H, d, $J = 3.2$ Hz), 6.61 (0.5 H, d, $J = 3.2$ Hz), 7.00–7.15 (3 H, m), 7.25–7.41 (3 H, m), 8.07 (0.5 H, s), 8.08 (0.5 H, s). HRMS: calcd

for $C_{22}H_{28}N_5O_2$ (MH^+) 394.2238, found 394.2239. To this compound (1.5 g, 3.81 mmol) dissolved in 75 mL of ethanol was added 2.6 g (1.9 mmol) of 20% $Pd(OH)_2$ on carbon (50% water), and the resulting mixture was agitated under a 50 psi atmosphere of hydrogen gas for 48 h (catalyst was recharged once during this time frame). The reaction mixture was filtered through Celite and concentrated to dryness to produce 720 mg of crude product, which was purified by flash chromatography (silica gel; 10% methanol in dichloromethane) affording 480 mg (42%) of compound **17d** as a colorless glass. LRMS: m/z 304.2 (MH^+). 1H NMR (400 MHz) ($CDCl_3$) (amide rotomers) δ : 1.00–1.13 (3 H, m), 1.61–1.77 (1 H, m), 1.82–1.98 (1 H, m), 3.22–3.47 (2 H, m), 3.41 (3 H, s), 3.65 (1 H, q, $J = 7.2$ Hz), 3.71–3.85 (2 H, m), 4.09–4.28 (1 H, m), 4.22 (2 H, s), 5.05–5.22 (1 H, m), 6.52 (1 H, s), 7.05 (0.5 H, d, $J = 3.2$ Hz), 7.08 (0.5 H, d, $J = 3.2$ Hz), 8.25 (0.5 H, s), 8.27 (0.5 H, s), 10.80 (1 H, br s). ^{13}C NMR (400 MHz) ($CDCl_3$) δ : 14.0, 14.9, 30.4, 31.4, 31.8, 32.2, 34.4, 35.1, 40.0, 40.6, 42.6, 44.9, 52.8, 53.0, 60.0, 102.3, 102.4, 103.0, 120.2, 120.4, 150.4, 150.6, 157.7, 157.8, 170.3, 170.4. HRMS: calcd for $C_{15}H_{22}N_5O_2$ (MH^+) 304.1767, found 304.1764.

cis-(5-Chloro-2,3-dihydrobenzofuran-2-yl)(4-methyl-3-(methyl(7H-pyrrolo[2,3-d]pyrimidin-4-yl)amino)piperidin-1-yl)methanone (18a). To a stirred solution of *cis-N*-methyl-*N*-(4-methylpiperidin-3-yl)-7H-pyrrolo[2,3-d]pyrimidin-4-amine (50 mg/0.20 mmol) and 5-chloro-2,3-dihydrobenzofuran-2-carboxylic acid (50 mg/0.25 mmol) in 6 mL of dimethylformamide cooled to 0 °C was added 40 mg (0.21 mmol) of 1-ethyl-3-(3-dimethylaminopropyl)carbodiimide hydrochloride, and the resulting mixture was warmed to room temperature and stirred for 16 h, at which point the reaction mixture was partitioned between dichloromethane and saturated $NaHCO_3$. The aqueous layer was extracted a second time with dichloromethane, and the combined dichloromethane layers were dried over $MgSO_4$, filtered through Celite, and concentrated to dryness *in vacuo*. The crude product was then purified by preparative TLC (silica gel; 19:1 dichloromethane/methanol) affording 22 mg (26%) of **18a** as a colorless oil (~3:1 mixture of diastereomers). LRMS: m/z 426.3 (MH^+). 1H NMR (400 MHz) ($CDCl_3$) δ : 0.85–1.00 (0.75 H, m), 1.05–1.18 (2.25 H, m), 1.83–2.13 (1 H, m), 2.43–2.71 (1 H, m), 3.15–3.42 (3 H, m), 3.44 (0.75 H, s), 3.48 (2.25 H, s), 3.53–4.27 (4 H, m), 5.21 (1 H, br s), 5.38 (1 H, dd, $J = 7.6$ Hz, $J = 2.4$ Hz), 5.46 (1 H, dd, $J = 7.6$ Hz, $J = 2.4$ Hz), 6.39–6.78 (2 H, m), 6.90–7.36 (3 H, m), 8.23–8.35 (1 H, m).

Compounds **18b** through **18m** were prepared in an analogous manner to that described for **17a**. The NMR data for these indicate the presence of amide rotamers.

1-Benzyl-3-(4-methyl-3-(methyl(7H-pyrrolo[2,3-d]pyrimidin-4-yl)amino)piperidine-1-carbonyl)pyrrolidin-2-one (18b). Liquid chromatography mass spectrometry (LCMS): m/z 447.4 (MH^+). 1H NMR (400 MHz) (CD_3OD) δ : 0.81–1.26 (4 H, m), 1.54–1.65 (1 H, m), 1.73–1.92 (1 H, m), 2.40 (1 H, br s), 2.52–2.80 (2 H, m), 3.20 (1.5 H, s), 3.25 (1.5 H, s), 3.29–3.98 (6 H, m), 4.31–4.52 (2 H, m), 6.54–6.64 (1 H, m), 7.04–7.07 (1 H, m), 7.15–7.33 (5 H, m), 8.04–8.06 (1 H, m).

cis-2-Cyclopentyl-1-(4-methyl-3-(methyl(7H-pyrrolo[2,3-d]pyrimidin-4-yl)amino)piperidin-1-yl)ethanone (18c). Amide rotamers. LRMS: m/z 356.2 (MH^+). 1H NMR (400 MHz) ($CDCl_3$) δ : 1.01 (3 H, s), 0.90–1.18 (2 H, m), 1.37–1.89 (7 H, m), 1.67 (2 H, s), 2.15–2.50 (4 H, m), 3.30 (1.5 H, s), 3.35 (1.5 H, s), 3.47 (1 H, s), 3.77 (2 H, br s), 3.78 (0.5 H, t, $J = 6.8$ Hz), 4.07 (0.5 H, d, $J = 11.6$ Hz), 4.95 (0.5 H, s), 5.05 (0.5 H, s), 6.46 (1 H, s), 6.97 (1 H, d, $J = 14.0$ Hz), 8.22 (1 H, d, $J = 11.2$ Hz), 10.15 (0.5 H, br s), 10.22 (0.5 H, br s). ^{13}C NMR (400 MHz) ($CDCl_3$) δ : 14.1, 14.9, 24.9, 25.0, 30.7, 31.9, 31.9, 32.4, 32.7, 32.8, 34.3, 35.0, 36.6, 36.8, 39.0, 39.4, 39.5, 41.7, 42.7, 47.1, 53.3, 102.3, 102.4, 102.8, 119.7, 120.1, 150.8, 150.9, 151.7, 152.0, 157.8, 157.9, 171.4, 171.6. HRMS: calcd for $C_{20}H_{30}N_5O$ (MH^+) 356.2445, found 356.2438.

3-(4-Methyl-3-(methyl(7H-pyrrolo[2,3-d]pyrimidin-4-yl)amino)-piperidine-1-carbonyl)cyclopentanone (18d). LCMS: m/z 356.4

(MH^+). 1H NMR (400 MHz) (CD_3OD) δ : 0.81–0.93 (1 H, m), 1.02–1.15 (2 H, m), 1.60–1.75 (1 H, m), 1.82–1.94 (1 H, m), 2.00–2.52 (5 H, m), 3.03–3.12 (1 H, m), 3.27 (2 H, s), 3.39 (1 H, s), 3.46–3.63 (2 H, m), 3.68–3.73 (1 H, m), 3.80–4.02 (2 H, m), 4.95 (1 H, br s), 6.59–6.60 (1 H, m), 7.05–7.07 (1 H, m), 8.06 (0.7 H, s), 8.09 (0.3 H, s).

(4-Methyl-3-(methyl(7H-pyrrolo[2,3-d]pyrimidin-4-yl)amino)-piperidin-1-yl)(thiophen-3-yl)methanone (18e). LRMS: m/z 356.3 (MH^+). 1H NMR (400 MHz) ($CDCl_3$) δ : 0.95–1.15 (4 H, m), 1.22–1.34 (1 H, m), 1.68 (2 H, br s), 3.40 (3 H, s), 3.63 (2 H, br s), 3.85 (2 H, t, $J = 8.8$ Hz), 5.13 (1 H, br s), 6.54 (1 H, d, $J = 3.6$ Hz), 7.05 (1 H, d, $J = 4.0$ Hz), 7.19 (1 H, d, $J = 5.6$ Hz), 7.30 (1 H, br s), 7.53 (1 H, s), 8.28 (1 H, s).

(4-Methyl-3-(methyl(7H-pyrrolo[2,3-d]pyrimidin-4-yl)amino)-piperidin-1-yl)(tetrahydrofuran-3-yl)methanone (18f). LRMS: m/z 344.2 (MH^+). 1H NMR (400 MHz) ($CDCl_3$) δ : 1.00–1.04 (3 H, m), 1.78 (1 H, br s), 1.75–1.80 (1 H, m), 1.81–2.51 (3 H, m), 3.10–3.34 (2 H, m), 3.23 (3 H, s), 3.40–3.91 (6 H, m), 4.05 (1 H, sp 1/2 ABq), 5.00 (1 H, 1/2 ABq, $J = 60$ Hz), 6.44 (1 H, d, $J = 10.4$ Hz), 7.00 (1 H, dd, $J = 16.0$ Hz, $J = 3.2$ Hz), 8.21 (0.5 H, s), 8.25 (0.5 H, s), 11.58 (0.5 H, s), 11.80 (0.5 H, s). ^{13}C NMR (400 MHz) ($CDCl_3$) δ : 13.9, 14.0, 14.7, 14.9, 30.0, 30.1, 30.3, 30.7, 31.8, 31.9, 32.0, 32.2, 32.3, 34.3, 35.1, 35.2, 39.4, 39.6, 41.2, 41.3, 41.5, 41.5, 42.1, 42.4, 46.7, 46.9, 53.3, 53.7, 68.4, 68.5, 70.5, 70.6, 70.7, 102.0, 102.1, 103.0, 103.1, 120.2, 120.6, 150.6, 151.9, 152.0, 157.7, 157.8, 171.3, 171.7. HRMS: calcd for $C_{18}H_{26}N_5O_2$ (MH^+) 344.2081, found 344.2075.

cis-Cyclopentyl(4-methyl-3-(methyl(7H-pyrrolo[2,3-d]pyrimidin-4-yl)amino)piperidin-1-yl)methanone (18g). LRMS: m/z 342.2 (MH^+). 1H NMR (400 MHz) ($CDCl_3$) δ : 0.95–1.05 (3 H, m), 1.38–1.88 (7 H, m), 2.37–2.38 (2 H, m), 2.79–2.89 (2 H, m), 3.29 (1.5 H, s), 3.35 (1.5 H, s), 3.52–3.68 (4 H, m), 3.82 (0.5 H, q, $J = 7.6$ Hz), 4.09 (0.5 H, d, $J = 10.4$ Hz), 4.93 (0.5 H, br s), 5.05 (0.5 H, br s), 6.44 (0.5 H, s), 6.46 (0.5 H, s), 6.98 (0.5 H, d, $J = 2.8$ Hz), 7.03 (0.5 H, d, $J = 2.8$ Hz), 8.21 (0.5 H, s), 8.25 (0.5 H, s), 11.26 (0.5 H, br s), 11.47 (0.5 H, br s). ^{13}C NMR (400 MHz) ($CDCl_3$) δ : 14.2, 14.9, 16.0, 30.1, 30.1, 30.4, 30.7, 32.0, 32.1, 32.5, 34.3, 35.1, 39.3, 41.1, 41.4, 42.1, 42.5, 46.9, 53.3, 102.1, 102.3, 102.9, 120.0, 120.4, 150.7, 151.9, 157.8, 174.6, 175.0. HRMS: calcd for $C_{19}H_{28}N_5O$ (MH^+) 342.2288, found 342.2280.

1-(4-Methyl-3-(methyl(7H-pyrrolo[2,3-d]pyrimidin-4-yl)amino)-piperidin-1-yl)-2-(methylsulfonyl)ethanone (18h). LCMS: m/z 366.2 (MH^+). 1H NMR (400 MHz) (CD_3OD) δ : 1.05 (2 H, d, $J = 6.8$ Hz), 1.11 (1 H, d, $J = 7.2$ Hz), 1.61–1.95 (2 H, m), 2.06–2.15 (1 H, m), 1.40–1.53 (1 H, m), 3.11 (2 H, s), 3.13 (1 H, s), 3.59–3.68 (1 H, m), 3.80–4.09 (2 H, m), 4.35–4.63 (2 H, m), 4.99–5.12 (1 H, m), 6.62 (1 H, d, $J = 3.6$ Hz), 7.08–7.89 (1 H, m), 8.10 (0.6 H, s), 8.15 (0.4 H, s).

cis-2-Cyclopropyl-1-(4-methyl-3-(methyl(7H-pyrrolo[2,3-d]pyrimidin-4-yl)amino)piperidin-1-yl)ethanone (18i). LRMS: m/z 328.2 (MH^+). 1H NMR (400 MHz) ($CDCl_3$) δ : –0.01–0.04 (2 H, m), 0.24–0.41 (2 H, m), 0.78–0.94 (3 H, m), 1.48 (1 H, br s), 1.59–1.76 (1 H, m), 1.94–2.38 (4 H, m), 3.16 (1.5 H, s), 3.20 (1.5 H, s), 3.31 (1 H, d, $J = 4.8$ Hz), 3.39–3.58 (2 H, m), 3.59–3.68 (0.5 H, m), 3.93 (0.5 H, d, $J = 9.6$ Hz), 4.82 (0.5 H, br s), 4.92 (0.5 H, br s), 6.31 (0.5 H, s), 6.32 (0.5 H, s), 6.85 (0.5 H, d, $J = 3.2$ Hz), 6.89 (0.5 H, d, $J = 2.8$ Hz), 8.07 (0.5 H, s), 8.10 (0.5 H, s), 11.17 (0.5 H, br s), 11.37 (0.5 H, br s). ^{13}C NMR (400 MHz) ($CDCl_3$) δ : 4.5, 4.7, 7.3, 7.4, 14.1, 14.9, 30.6, 31.9, 32.0, 32.4, 34.3, 35.0, 38.7, 38.9, 39.1, 41.8, 42.8, 47.1, 53.2, 53.5, 102.1, 102.3, 102.9, 120.1, 120.4, 150.7, 151.9, 152.0, 157.8, 157.9, 171.3, 171.5. HRMS: calcd for $C_{18}H_{26}N_5O$ (MH^+) 328.2132, found 328.2124.

cis-3,3,3-Trifluoro-1-(4-methyl-3-(methyl(7H-pyrrolo[2,3-d]pyrimidin-4-yl)amino)piperidin-1-yl)propan-1-one (18j). LRMS: m/z 356.2 (MH^+). 1H NMR (400 MHz) ($CDCl_3$) δ TMS: 0.97 (1.5 H, d, $J = 7.2$ Hz), 1.08 (1.5 H, d, $J = 7.2$ Hz), 1.60–1.70 (1 H, m), 1.79–1.94 (1 H, m), 2.37–2.50 (1 H, m), 3.14–3.37 (2 H, m), 3.20 (1.5 H, s), 3.35 (1.5 H, s), 3.40–3.62 (2 H, m), 3.72 (1 H, q, $J = 12.8$ Hz), 3.70–3.86 (0.5 H, m), 4.06 (0.5 H, d, $J = 8.8$ Hz), 5.05 (1 H, br s), 6.46 (0.5 H, d, $J = 3.6$ Hz), 6.47 (0.5 H,

d, $J = 5.2$ Hz), 6.99 (0.5 H, d, $J = 3.2$ Hz), 7.04 (0.5 H, d, $J = 3.2$ Hz), 8.21 (0.5 H, s), 8.24 (0.5 H, s), 10.96 (1 H, br s), 11.15 (0.5 H, br s). ^{13}C NMR (400 MHz) (CDCl_3) δ : 13.1, 13.6, 29.5, 29.9, 30.5, 30.8, 30.9, 33.3, 34.0, 36.9, 37.2, 37.5, 38.3, 41.4, 42.8, 46.3, 49.7, 51.7, 52.5, 101.0, 101.3, 101.9, 102.0, 119.1, 119.5, 121.8, 124.5, 149.6, 149.7, 150.9, 151.0, 156.7, 160.6, 161.0, 206.1. HRMS: calcd for $\text{C}_{16}\text{H}_{21}\text{F}_3\text{N}_5\text{O}$ (MH^+) 356.1693, found 356.1689.

2,2-Dimethyl-3-(4-methyl-3-(methyl(7*H*-pyrrolo[2,3-*d*]pyrimidin-4-yl)amino)piperidin-1-yl)-3-oxopropanenitrile (18k). LRMS: m/z 341.3 (MH^+). ^1H NMR (400 MHz) (CDCl_3) δ : 1.09 (3 H, d, $J = 7.2$ Hz), 1.63 (6 H, s), 1.79 (1 H, br s), 1.99–2.16 (1 H, m), 2.51–2.57 (1 H, m), 3.28–3.42 (1 H, m), 3.42 (3 H, s), 3.88 (2 H, br s), 4.07 (1 H, d, $J = 8.4$ Hz), 5.15 (1 H, br s), 6.57 (1 H, d, $J = 3.6$ Hz), 7.09 (1 H, d, $J = 3.2$ Hz), 8.28 (1 H, s).

2-Methyl-3-(4-methyl-3-(methyl(7*H*-pyrrolo[2,3-*d*]pyrimidin-4-yl)amino)piperidin-1-yl)-3-oxopropanenitrile (18l). LCMS: m/z 327.3 (MH^+). ^1H NMR (400 MHz) (CDCl_3) δ : 1.03–1.11 (3 H, m), 1.51–1.56 (3 H, m), 1.61 (1 H, br s), 1.78–1.96 (1 H, m), 2.08 (1 H, br s), 3.34 (1 H, s), 3.39 (2 H, s), 3.40–3.59 (1 H, m), 3.60–3.81 (2 H, m), 3.81–4.10 (1.5 H, m), 4.21 (1/2 H, d, $J = 13.2$ Hz), 5.03 (1/2 H, br s), 5.10 (1/2 H, br s), 5.20 (1 H, br s), 6.51 (1/3 H, d, $J = 3.2$ Hz), 6.55 (2/3 H, d, $J = 3.6$ Hz), 7.05 (1 H, d, $J = 3.6$ Hz), 8.23 (1/3 H, s), 8.25 (2/3 H, s).

cis-3-(4-Methyl-3-(methyl(7*H*-pyrrolo[2,3-*d*]pyrimidin-4-yl)amino)piperidin-1-yl)-3-oxopropanenitrile (18m). LRMS: m/z 313.3 (MH^+). ^1H NMR (400 MHz) (CDCl_3) δ : 1.08 (1.5 H, d, $J = 7.2$ Hz), 1.10 (1.5 H, d, $J = 7.2$ Hz), 1.63–2.09 (2 H, m), 2.42–2.58 (1 H, m), 3.26–3.68 (2 H, m), 3.41 (1.5 H, s), 3.46 (1.5 H, s), 3.56 (2 H, s), 3.70–3.92 (1.5 H, m), 4.09 (0.5 H, dd, $J = 8.8$ Hz, $J = 4.4$ Hz), 5.16 (1 H, br s), 6.57 (1 H, t, $J = 3.6$ Hz), 7.10 (1 H, t, $J = 3.6$ Hz), 8.26 (1 H, s). HRMS: calcd for $\text{C}_{16}\text{H}_{21}\text{N}_6\text{O}$ (MH^+) 313.1771, found 313.1776.

((*S*)-3-Hydroxypyrrolidin-1-yl)((*3*R*,4*R)-4-methyl-3-(methyl(7*H*-pyrrolo[2,3-*d*]pyrimidin-4-yl)amino)piperidin-1-yl)methanone (20).** To a stirred solution of (*S*)-pyrrolidin-3-ol (1.0 g/11.5 mmol) dissolved in 15 mL of dichloromethane and cooled to 0 °C was added 2.3 g (11.5 mmol) of 4-nitrophenylchloroformate followed by 1.6 mL (11.5 mmol) of triethylamine, and the resulting mixture was stirred at 0 °C for 1.5 h. The reaction mixture was then partitioned between water and chloroform, the aqueous layer was extracted 3 × 50 mL with chloroform, and the combined chloroform layers were dried over MgSO_4 , filtered through Celite, and concentrated to dryness *in vacuo* affording 2.9 g (quant) of the intermediate (*S*)-4-nitrophenyl 3-hydroxypyrrolidine-1-carboxylate as a yellow solid. LRMS: m/z 253.2 (MH^+). ^1H NMR (400 MHz) (CDCl_3) δ : 1.97–2.16 (2 H, m), 3.48–3.80 (4 H, m), 4.56–4.60 (1 H, m), 7.33 (2 H, dd, $J = 6.8$ Hz, $J = 2.4$ Hz), 8.25 (2 H, d, $J = 8.8$ Hz). HRMS: calcd for $\text{C}_{11}\text{H}_{13}\text{N}_2\text{O}_5$ (MH^+) 253.0819, found 253.0817. Separately, *N*-methyl-*N*-((*3*R*,4*R**)-4-methylpiperidin-3-yl)-7*H*-pyrrolo[2,3-*d*]pyrimidin-4-amine (50 mg/0.20 mmol), prepared from **19a** as described above, dissolved in 5 mL of *tert*-butanol, was charged to a pressure tube along with 76 mg (0.30 mmol) of (*S*)-4-nitrophenyl 3-hydroxypyrrolidine-1-carboxylate and 0.5 mL of triethylamine, and the sealed tube then heated at 100 °C for 48 h. After being cooled to room temperature the reaction mixture was partitioned between chloroform and saturated NaHCO_3 . The aqueous layer was extracted 3 × 30 mL with chloroform, and the combined chloroform layers were dried over Na_2SO_4 , filtered through Celite, and concentrated to dryness *in vacuo*. The crude product was then purified by flash chromatography (silica gel; 10–15% methanol in chloroform). The product was then triturated with chloroform/hexanes to yield 24 mg (33%) of **20** as an off-white solid after drying. LRMS: m/z 359.2 (MH^+). ^1H NMR (400 MHz) (CDCl_3) δ : 1.03 (3 H, d, $J = 6.8$ Hz), 1.60 (1 H, d, $J = 10.8$ Hz), 1.93 (2 H, br s), 2.45 (1 H, t, $J = 5.2$ Hz), 3.22 (1 H, t, $J = 10.8$ Hz), 3.36 (3 H, s), 3.37–3.71 (8 H, m), 4.44 (1 H, s), 4.94 (1 H, br s), 6.46 (1 H, s), 7.04 (1 H, d, $J = 3.6$ Hz), 8.20 (1 H, s), 11.81 (1 H, br s). ^{13}C NMR (400 MHz) (CDCl_3) δ : 13.8, 31.2, 31.5, 33.9, 34.9, 43.1, 45.5, 46.2, 54.8, 56.5, 70.4, 102.8, 102.9, 121.1, 147.3,

147.4, 157.6, 163.2. HRMS: calcd for $\text{C}_{18}\text{H}_{27}\text{N}_6\text{O}_2$ (MH^+) 359.2190, found 359.2188.

Acknowledgment. This research was sponsored by Pfizer Inc. The authors gratefully acknowledge Dr. Gary Chan MD and Dr. Samuel Zwillich MD for helpful conversations and for providing summaries of clinical results for **1** citrate relating to the prevention of renal allograft rejection and treatment of rheumatoid arthritis, respectively. The authors also acknowledge Daniel Virtue and Melissa Rockwell for chiral separations performed, Matthew Teague for high-resolution mass spectra, and Jon Bordner and Ivan Samardjiev for the single crystal X-ray structure of compound **20**. The support provided by Martin Goulding at Complete Medical Communications, funded by Pfizer Inc., consisted solely of manuscript editing and formatting, and no contribution was made to editorial content.

Supporting Information Available: Additional HSA compounds (**6c**, S1–S63), with initial JAK3% inhibition data. This material is available free of charge via the Internet at <http://pubs.acs.org>.

References

- (1) Stock, P. G. The year in review—ATC 2002. *Am. J. Transplant.* **2003**, *3*, 373–380.
- (2) Hong, J. C.; Kahan, B. D. Immunosuppressive agents in organ transplantation: past, present, and future. *Semin. Nephrol.* **2000**, *20*, 108–125.
- (3) Darnell, J. E. J.; Kerr, I. M.; Stark, G. R. Jak-STAT pathways and transcriptional activation in response to IFNs and other extracellular signaling proteins. *Science* **1994**, *264*, 1415–1421.
- (4) Ghoreschi, K.; Laurence, A.; O'Shea, J. J. Selectivity and therapeutic inhibition of kinases: to be or not to be? *Nat. Immunol.* **2009**, *10*, 356–360.
- (5) Ghoreschi, K.; Laurence, A.; O'Shea, J. J. Janus kinases in immune cell signaling. *Immunol. Rev.* **2009**, *228*, 273–287.
- (6) Johnston, J. A.; Bacon, C. M.; Riedy, M. C.; O'Shea, J. J. Signaling by IL-2 and related cytokines: JAKs, STATs and relationship to immunodeficiency. *J. Leukocyte Biol.* **1996**, *60*, 441–452.
- (7) Oakes, S. A.; Candotti, F.; Johnston, J. A.; Chen, Y. Q.; Ryan, J. J.; Taylor, N.; Liu, X.; Henninghausen, L.; Notarangelo, L. D.; Paul, W. E.; Blaese, R. M.; O'Shea, J. J. Signaling via IL-2 and IL-4 in JAK3-deficient severe combined immunodeficiency lymphocytes: JAK3-dependent and independent pathways. *Immunity* **1996**, *5*, 605–615.
- (8) Chen, M.; Cheng, A.; Chen, Y. Q.; Hymel, A.; Hanson, E. P.; Kimmel, L.; Minami, Y.; Taniguchi, T.; Changelian, P. S.; O'Shea, J. J. The amino terminus of JAK3 is necessary and sufficient for binding to the common gamma chain and confers the ability to transmit interleukin 2-mediated signals. *Proc. Natl. Acad. Sci. U.S.A.* **1997**, *94*, 6910–6915.
- (9) Hofmann, S. R.; Ettinger, R.; Zhou, Y. J.; Gadina, M.; Lipsky, P.; Siegel, R.; Candotti, F.; O'Shea, J. J. Cytokines and their role in lymphoid development, differentiation and homeostasis. *Curr. Opin. Allergy Clin. Immunol.* **2002**, *2*, 495–506.
- (10) Macchi, P.; Villa, A.; Giliani, S.; Sacco, M. G.; Frattini, A.; Porta, F.; Ugazio, A. G.; Johnston, J. A.; Candotti, F.; O'Shea, J. J. Mutations of Jak-3 gene in patients with autosomal severe combined immunodeficiency (SCID). *Nature* **1995**, *377*, 65–68.
- (11) Noguchi, M.; Rosenblatt, H. M.; Filipovich, A. H.; Adelstein, S.; Modi, W. S.; McBride, O. W.; Leonard, W. J. Interleukin-2 receptor gamma chain mutation results in X-linked severe combined immunodeficiency in humans. *Cell* **1993**, *73*, 147–157.
- (12) Russell, S. M.; Tayebi, N.; Nakajima, H.; Riedy, M. C.; Roberts, J. L.; Aman, M. J.; Migone, T. S.; Noguchi, M.; Markert, M. L.; Buckley, R. H.; O'Shea, J. J.; Leonard, W. J. Mutation of Jak3 in a patient with SCID: essential role of Jak3 in lymphoid development. *Science* **1995**, *270*, 797–800.
- (13) Pesu, M.; Candotti, F.; Husa, M.; Hofmann, S. R.; Notarangelo, L. D.; O'Shea, J. J. Jak3, severe combined immunodeficiency, and a new class of immunosuppressive drugs. *Immunol. Rev.* **2005**, *203*, 127–142.
- (14) Changelian, P. S.; Flanagan, M. E.; Ball, D. J.; Kent, C. R.; Magnuson, K. S.; Martin, W. H.; Rizzuti, B. J.; Sawyer, P. S.;

- Perry, B. D.; Brissette, W. H.; McCurdy, S. P.; Kudlacz, E. M.; Conklyn, M. J.; Elliott, E. A.; Koslov, E. R.; Fisher, M. B.; Strelevitz, T. J.; Yoon, K.; Whipple, D. A.; Sun, J.; Munchhof, M. J.; Doty, J. L.; Casavant, J. M.; Blumenkopf, T. A.; Hines, M.; Brown, M. F.; Lillie, B. M.; Subramanyam, C.; Shang-Poa, C.; Milici, A. J.; Beckius, G. E.; Moyer, J. D.; Su, C.; Woodworth, T. G.; Gaweco, A. S.; Beals, C. R.; Littman, B. H.; Fisher, D. A.; Smith, J. F.; Zagouras, P.; Magna, H. A.; Saltarelli, M. J.; Johnson, K. S.; Nelms, L. F.; Des Etages, S. G.; Hayes, L. S.; Kawabata, T. T.; Finco-Kent, D.; Baker, D. L.; Larson, M.; Si, M. S.; Paniagua, R.; Higgins, J.; Holm, B.; Reitz, B.; Zhou, Y. J.; Morris, R. E.; O'Shea, J. J.; Borie, D. C. Prevention of organ allograft rejection by a specific Janus kinase 3 inhibitor. *Science* **2003**, *302*, 875–878.
- (15) West, K. CP-690550, a JAK3 inhibitor as an immunosuppressant for the treatment of rheumatoid arthritis, transplant rejection, psoriasis and other immune-mediated disorders. *Curr. Opin. Invest. Drugs* **2009**, *10*, 491–504.
- (16) Sorbera, L. A.; Serradell, N.; Bolos, J.; Rosa, E.; Bozzo, J. CP-690,550. *Drugs Future* **2007**, *32*, 674–680.
- (17) Wroblewski, S. T.; Pitts, W. J. Chapter 12 Advances in the discovery of small molecule JAK3 inhibitors. *Annu. Rep. Med. Chem.* **2009**, *44*, 247–264.
- (18) Kudlacz, E.; Perry, B.; Sawyer, P.; Conklyn, M.; McCurdy, S.; Brissette, W.; Flanagan, A.; Changelian, P. The novel JAK-3 inhibitor CP-690550 is a potent immunosuppressive agent in various murine models. *Am. J. Transplant.* **2004**, *4*, 51–57.
- (19) Meyer, D. M.; Jesson, M. I.; Li, W.; Elrick, M. M.; Funckes-Shippy, C. L.; Warner, J. D.; Gross, C. J.; Dowty, M. E.; Ramaiah, S. K.; Hirsch, J. L.; Saabye, M. J.; Barks, J. L.; Kishore, N.; Morris, D. L. Anti-inflammatory activity and neutrophil reductions mediated by JAK1 and JAK3 inhibition in the rat AIA model. *J. Inflammation (London)* **2010**, *7*, 41.
- (20) Simonsen, J. *The Terpenes*; Cambridge University Press: Cambridge, 1953; pp 394–408.
- (21) Brown Ripin, D. H.; Abele, S.; Cai, W.; Blumenkopf, T.; Casavant, J. M.; Doty, J. L.; Flanagan, M.; Koecher, C.; Laue, K. W.; McCarthy, K.; Meltz, C.; Munchhof, M. J.; Pouwer, K.; Sha, B.; Sun, J.; Teixeira, J.; Vries, T.; Whipple, D. A.; Wilcox, G. Development of a scalable route for the production of *cis*-N-benzyl-3-methylamino-4-methylpiperidine. *Org. Process Res. Dev.* **2003**, *7*, 115–120.
- (22) Jiang, J. K.; Ghoreschi, K.; Deflorian, F.; Chen, Z.; Perreira, M.; Pesu, M.; Smith, J.; Nguyen, D. T.; Liu, E. H.; Leister, W.; Costanzi, S.; O'Shea, J. J.; Thomas, C. J. Examining the chirality, conformation and selective kinase inhibition of 3-((3R,4R)-4-methyl-3-(methyl(7H-pyrrolo[2,3-d]pyrimidin-4-yl)amino)piperidin-1-yl)-3-oxopropanenitrile (CP-690,550). *J. Med. Chem.* **2008**, *51*, 8012–8018.
- (23) Williams, N. K.; Bamert, R. S.; Patel, O.; Wang, C.; Walden, P. M.; Wilks, A. F.; Fantino, E.; Rossjohn, J.; Lucet, I. S. Dissecting specificity in the Janus kinases: the structures of JAK-specific inhibitors complexed to the JAK1 and JAK2 protein tyrosine kinase domains. *J. Mol. Biol.* **2009**, *387*, 219–232.
- (24) Chrencik, J. E.; Patny, A.; Leung, I. K.; Korniski, B.; Emmons, T. L.; Hall, T.; Weinberg, R. A.; Gormley, J. A.; Williams, J. M.; Day, J. E.; Hirsch, J. L.; Kiefer, J. R.; Leone, J. W.; Fischer, H. D.; Sommers, C. D.; Huang, H. C.; Jacobsen, E. J.; Tenbrink, R. E.; Tomasselli, A. G.; Benson, T. E. Structural and thermodynamic characterization of the TYK2 and JAK3 kinase domains in complex with CP-690550 and CMP-6. *J. Mol. Biol.* **2010**, *400*, 413–433.
- (25) World Intellectual Property Organization. (WO/2003/048162) Novel Crystalline Compound. <http://www.wipo.int/pctdb/en/wo.jsp?wo=2003048162&IA=IB2002004948&DISPLAY=DOCS>. Accessed 3 August 2010.
- (26) van Gurp, E.; Weimar, W.; Gaston, R.; Brennan, D.; Mendez, R.; Prusch, J.; Swan, S.; Pescovitz, M. D.; Ni, G.; Wang, C.; Krishnaswami, S.; Chow, V.; Chan, G. Phase 1 dose-escalation study of CP-690-550 in stable renal allograft recipients: preliminary findings of safety, tolerability, effects on lymphocyte subsets and pharmacokinetics. *Am. J. Transplant.* **2008**, *8*, 1711–1718.
- (27) Lawendy, N.; Krishnaswami, S.; Wang, R.; Gruben, D.; Cannon, C.; Swan, S.; Chan, G. Effect of CP-690,550, an orally active janus kinase inhibitor, on renal function in healthy adult volunteers. *J. Clin. Pharmacol.* **2009**, *49*, 423–429.
- (28) Dalvie, D.; Obach, R. S.; Kang, P.; Prakash, C.; Loi, C. M.; Hurst, S.; Nedderman, A.; Goulet, L.; Smith, E.; Bu, H. Z.; Smith, D. A. Assessment of three human in vitro systems in the generation of major human excretory and circulating metabolites. *Chem. Res. Toxicol.* **2009**, *22*, 357–368.
- (29) Karaman, M. W.; Herrgard, S.; Treiber, D. K.; Gallant, P.; Atteridge, C. E.; Campbell, B. T.; Chan, K. W.; Ciceri, P.; Davis, M. I.; Edeen, P. T.; Faraoni, R.; Filloyd, M.; Hunt, J. P.; Lockhart, D. J.; Milanov, Z. V.; Morrison, M. J.; Pallares, G.; Patel, H. K.; Pritchard, S.; Wodicka, L. M.; Zarrinkar, P. P. A qualitative analysis of kinase inhibitor selectivity. *Nat. Biotechnol.* **2008**, *26*, 127–132.
- (30) Pfizer Inc. Data on file, 2009.
- (31) Borie, D. C.; Larson, M. J.; Flores, M. G.; Campbell, A.; Rousvoal, G.; Zhang, S.; Higgins, J. P.; Ball, D. J.; Kudlacz, E. M.; Brissette, W. H.; Elliott, E. A.; Reitz, B. A.; Changelian, P. S. Combined use of the JAK3 inhibitor CP-690,550 with mycophenolate mofetil to prevent kidney allograft rejection in nonhuman primates. *Transplantation* **2005**, *80*, 1756–1764.
- (32) Rousvoal, G.; Si, M. S.; Lau, M.; Zhang, S.; Berry, G. J.; Flores, M. G.; Changelian, P. S.; Reitz, B. A.; Borie, D. C. Janus kinase 3 inhibition with CP-690,550 prevents allograft vasculopathy. *Transplant Int.* **2006**, *19*, 1014–1021.
- (33) Busque, S.; Leventhal, J.; Brennan, D.; Steinberg, S.; Klintmalm, G.; Shah, T.; Mulgaonkar, S.; Bromberg, J.; Vincenti, F.; Hariharan, S.; Slakey, D.; Peddi, V. R.; Fisher, R. A.; Lawendy, N.; Wang, C.; Chan, G. Calcineurin-inhibitor-free immunosuppression based on the JAK inhibitor CP690,550: a pilot study in de novo kidney allograft recipients. *Am. J. Transplant.* **2009**, *9*, 1936–1945.
- (34) Milici, A. J.; Kudlacz, E. M.; Audoly, L.; Zwillich, S.; Changelian, P. Cartilage preservation by inhibition of Janus kinase 3 in two rodent models of rheumatoid arthritis. *Arthritis Res. Ther.* **2008**, *10*, R14.
- (35) Kremer, J. M.; Bloom, B. J.; Breedveld, F. C.; Coombs, J. H.; Fletcher, M. P.; Gruben, D.; Krishnaswami, S.; Burgos-Vargas, R.; Wilkinson, B.; Zerbini, C. A. F.; Zwillich, S. H. The safety and efficacy of a JAK inhibitor in patients with active rheumatoid arthritis: results of a double-blind, placebo-controlled phase IIa trial of three dose levels of CP-690,550 versus placebo. *Arthritis Rheum.* **2009**, *60*, 1895–1905.
- (36) Kremer, J. M.; Cohen, S.; Wilkinson, B.; Connell, C.; French, J.; Gomez Reino, J.; Gruben, D.; Kanik, K.; Krishnaswami, S.; Pascual-Ramos, V.; Wallenstein, G.; Zwillich, S. The oral JAK inhibitor CP-690,550 (CP) in combination with methotrexate (MTX) is efficacious, safe and well tolerated in patients with active rheumatoid arthritis (RA) with an inadequate response to methotrexate alone. *Arthritis Rheum.* **2008**, *58*, 4030.
- (37) Kremer, J. M.; Cohen, S.; Wilkinson, B.; Gruben, D.; Wallenstein, G.; Kanik, K.; Zwillich, S. H. Safety and efficacy after 24 week (WK) dosing of the oral JAK inhibitor CP-690,550 (CP) in combination with methotrexate (MTX) in patients (PTS) with active rheumatoid arthritis (RA). *Arthritis Rheum.* **2009**, *60* (Suppl. 10), S719, 1925 (abstract).
- (38) Kanik, K.; Fleischmann, R.; Cutolo, M.; Genovese, M.; Lee, E.; Sadis, S.; Connell, C.; Gruben, D.; Krishnaswami, S.; Wallenstein, G.; Wilkinson, B.; Zwillich, S. Phase 2b dose ranging monotherapy study of the oral JAK inhibitor CP-690,550 (CP) or adalimumab (ADA) vs placebo (PBO) in patients (pts) with active rheumatoid arthritis (RA) with an inadequate response to DMARDs. *Ann. Rheum. Dis.* **2009**, *68* (Suppl. 3), 123, OP-0159 (abstract).
- (39) Fleischmann, R. M.; Genovese, M. C.; Gruben, D.; Kanik, K.; Wallenstein, G.; Wilkinson, B.; Zwillich, S. H. Safety and efficacy after 24 week (wk) dosing of the oral JAK inhibitor CP-690,550 (CP) as monotherapy in patients (pts) with active rheumatoid arthritis (RA). *Arthritis Rheum.* **2009**, *60* (Suppl. 10), S718, 1924 (abstract).
- (40) Kalgutkar, A. S.; Choo, E.; Taylor, T. J.; Marfat, A. Disposition of CP-671,305, a selective phosphodiesterase 4 inhibitor in preclinical species. *Xenobiotica* **2004**, *34*, 755–770.
- (41) Obach, R. S. Inhibition of human cytochrome P450 enzymes by constituents of St. John's wort, an herbal preparation used in the treatment of depression. *J. Pharmacol. Exp. Ther.* **2000**, *294*, 88–95.
- (42) Kalgutkar, A. S.; Hatch, H. L.; Kosea, F.; Nguyen, H. T.; Choo, E. F.; McClure, K. F.; Taylor, T. J.; Henne, K. R.; Kuperman, A. V.; Dombroski, M. A.; Letavic, M. A. Preclinical pharmacokinetics and metabolism of 6-(4-(2,5-difluorophenyl)oxazol-5-yl)-3-isopropyl-1,2,4-triazolo[4,3-a]pyridine, a novel and selective p38alpha inhibitor: identification of an active metabolite in pre-clinical species and human liver microsomes. *Biopharm. Drug Dispos.* **2006**, *27*, 371–386.
- (43) Davoll, J. Pyrrolo[2,3-d]pyrimidines. *J. Chem. Soc.* **1960**, *82*, 131–138.